Article

Cell Reports

Non-Canonical Hedgehog Signaling Is a Positive Regulator of the WNT Pathway and Is Required for the Survival of Colon Cancer Stem Cells

Graphical Abstract

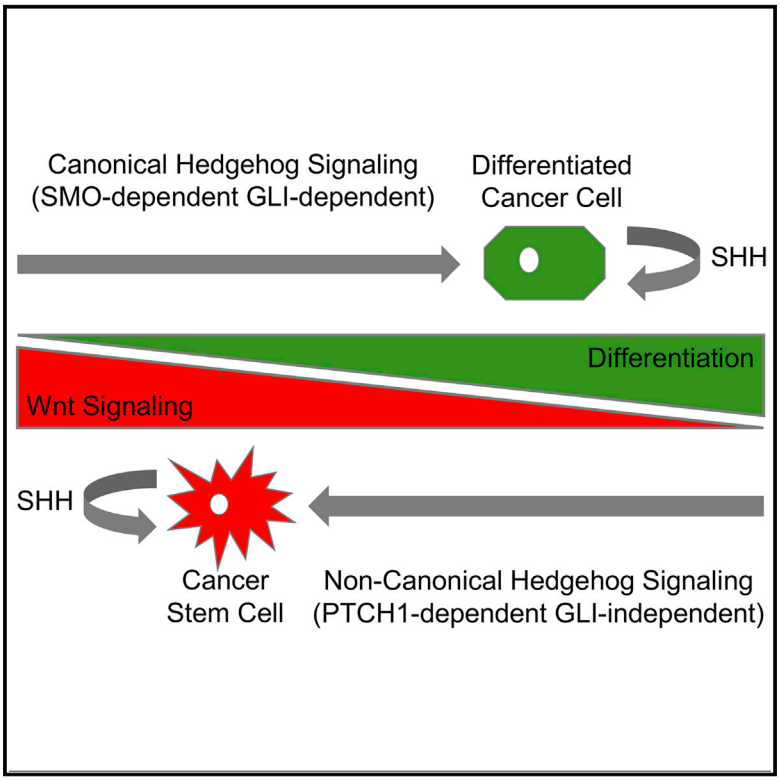

Authors

Joseph L. Regan, Dirk Schumacher, Stephanie Staudte, ..., Christian R.A. Regenbrecht, Reinhold Schäfer, Martin Lange

Correspondence

joseph.regan@charite.de (J.L.R.), martin.lange@bayer.com (M.L.)

In Brief

Colon cancer is a heterogeneous tumor driven by a subpopulation(s) of therapy-resistant cancer stem cells (CSCs). Regan et al. use 3D culture models to demonstrate that CSC survival is regulated by non-canonical, SHH-dependent, PTCH1-dependent Hedgehog signaling, which acts as a positive regulator of WNT signaling to block CSC differentiation.

Highlights

- Patient-derived colon cancer organoids are enriched for cancer stem cells (CSCs)
- Hedgehog signaling in CSCs is non-canonical, SHH dependent, and PTCH1 dependent
- Non-canonical Hedgehog signaling is a positive regulator of WNT signaling
- CSC survival is dependent on HHAT-mediated palmitoylation of SHH

Data and Software Availability

E-MTAB-5209

Regan et al., 2017, Cell Reports *21*, 2813–2828
December 5, 2017
https://doi.org/10.1016/j.celrep.2017.11.025

CellPress

Cell Reports
Article

OPEN ACCESS
CellPress

Non-Canonical Hedgehog Signaling Is a Positive Regulator of the WNT Pathway and Is Required for the Survival of Colon Cancer Stem Cells

Joseph L. Regan,[1,2,9,*] Dirk Schumacher,[3,4] Stephanie Staudte,[1,2] Andreas Steffen,[1] Johannes Haybaeck,[5,6] Ulrich Keilholz,[2] Caroline Schweiger,[6] Nicole Golob-Schwarzl,[6] Dominik Mumberg,[1] David Henderson,[1] Hans Lehrach,[7] Christian R.A. Regenbrecht,[2,8] Reinhold Schäfer,[2,3,4] and Martin Lange[1,*]

[1]Bayer AG, Drug Discovery, Pharmaceuticals, 13342 Berlin, Germany
[2]Charité Comprehensive Cancer Center, Charité – Universitätsmedizin Berlin, Charitéplatz 1, 10117 Berlin, Germany
[3]Laboratory of Molecular Tumor Pathology, Charité Universitätsmedizin Berlin, 10117 Berlin, Germany
[4]German Cancer Consortium (DKTK), DKFZ, Im Neuenheimer Feld 280, 69120 Heidelberg, Germany
[5]Department of Pathology, Medical Faculty, Otto von Guericke University Magdeburg, Leipziger Straße 44, Haus 28, 39120 Magdeburg, Germany
[6]Institute of Pathology, Medical University Graz, Auenbruggerplatz 25, 8036 Graz, Austria
[7]Max Planck Institute for Molecular Genetics, Ihnestrasse 73, 14195 Berlin, Germany
[8]cpo – cellular phenomics & oncology Berlin-Buch GmbH, Robert-Rössle-Straße 10, 13125 Berlin, Germany
[9]Lead Contact
*Correspondence: joseph.regan@charite.de (J.L.R.), martin.lange@bayer.com (M.L.)
https://doi.org/10.1016/j.celrep.2017.11.025

SUMMARY

Colon cancer is a heterogeneous tumor driven by a subpopulation of cancer stem cells (CSCs). To study CSCs in colon cancer, we used limiting dilution spheroid and serial xenotransplantation assays to functionally define the frequency of CSCs in a panel of patient-derived cancer organoids. These studies demonstrated cancer organoids to be enriched for CSCs, which varied in frequency between tumors. Whole-transcriptome analysis identified WNT and Hedgehog signaling components to be enhanced in CSC-enriched tumors and in aldehyde dehydrogenase (ALDH)-positive CSCs. Canonical GLI-dependent Hedgehog signaling is a negative regulator of WNT signaling in normal intestine and intestinal tumors. Here, we show that Hedgehog signaling in colon CSCs is autocrine SHH-dependent, non-canonical PTCH1 dependent, and GLI independent. In addition, using small-molecule inhibitors and RNAi against SHH-palmitoylating Hedgehog acyltransferase (HHAT), we demonstrate that non-canonical Hedgehog signaling is a positive regulator of WNT signaling and required for colon CSC survival.

INTRODUCTION

Colorectal cancer is a heterogeneous tumor that represents the third most common cancer and fourth most common cause of cancer deaths worldwide (Haggar and Boushey, 2009; Siegel et al., 2014). Recent data support a hierarchical model of colon cancer in which tumor growth is driven by a subpopulation of cancer stem cells (CSCs) that may also be the source of relapse following treatment (Reya et al., 2001; Shackleton et al., 2009; Ricci-Vitiani et al., 2007; O'Brien et al., 2007; Vermeulen et al., 2008). Elucidation of the molecular pathways that regulate CSC survival and contribute to tumor heterogeneity may therefore lead to more effective treatments.

Tumors recapitulate many of the cellular programs employed during the development of the tissue of origin (Karamboulas and Ailles, 2013; Reya et al., 2001). WNT and Hedgehog signaling frequently operate in unison to control cell growth, development, tissue homeostasis, and cancer (Taipale and Beachy, 2001; Song et al., 2015). In the intestine, WNT signaling is highest in the stem cell compartment at the crypt base, where it drives stem cell self-renewal, and decreases as cells move up through the intestinal crypt and into the differentiated area at the top of the crypt (Pinto et al., 2003).

Conversely, Hedgehog signaling in the colon is primarily confined to the differentiated cells at the top of the crypt, where it acts to antagonize WNT signaling and restrict its expression to the base of the crypt (Madison et al., 2005). Hedgehog signaling can be classified as either canonical or non-canonical. In canonical Hedgehog signaling, Hedgehog (SHH, IHH, or DHH) binds to its receptor PTCH1, which is also a direct target of Hedgehog signaling (Goodrich et al., 1996; Marigo and Tabin, 1996; Ingham, 1998; Kolterud et al., 2009; Scales and de Sauvage, 2009), to relieve it from its repression of SMO, which then activates a downstream signaling pathway, resulting in activation of the GLI family zinc-finger transcription factors GLI1, GLI2, and GLI3. These GLI proteins then translocate to the nucleus, where they regulate the transcription of several target genes. Non-canonical Hedgehog signaling is less well defined but generally refers to Hedgehog-dependent signals that do not act via the canonical Hedgehog-to-GLI route and includes any GLI-independent cellular and tissue responses (Brennan et al., 2012; Thibert et al., 2003; Polizio et al., 2011; Barnes et al., 2001; Testaz et al., 2001; Chinchilla et al., 2010). Two classes

of GLI-independent, non-canonical Hedgehog signaling have been described: type I non-canonical Hedgehog signaling, which works through PTCH1 and is independent of SMO, and type II, which functions through SMO (Brennan et al., 2012). In addition, SMO-independent GLI activation has also been referred to as non-canonical Hedgehog signaling (Petrova et al., 2015; Nolan-Stevaux et al., 2009).

Activating mutations in the WNT signaling pathway are found in 90% of colorectal cancers (Miyaki et al., 1994). Hedgehog genes, on the other hand, are rarely mutated in colorectal cancer (Cancer Genome Atlas Network, 2012) but are, instead, upregulated (Oniscu et al., 2004; Yoshikawa et al., 2009; Berman et al., 2003), and conflicting data suggest either a paracrine (Yauch et al., 2008) or autocrine pathway activation (Varnat et al., 2009). Crosstalk between WNT and Hedgehog signaling has been shown to be important in the development and progression of colon cancer (van den Brink et al., 2004; Van Dop et al., 2009; Akiyoshi et al., 2006; Song et al., 2015; van den Brink and Hardwick, 2006), and there are numerous avenues for molecular crosstalk between the two pathways (Briscoe and Thérond, 2013). Similar to the normal intestine, many studies report GLI-dependent canonical Hedgehog signaling to be a negative regulator of WNT signaling in colon cancer (van den Brink et al., 2004; Van Dop et al., 2009; Akiyoshi et al., 2006). Drugs that target the canonical Hedgehog signaling pathway in colon cancer, where WNT signaling drives proliferation, may therefore prove to be ineffective. Indeed, recent clinical trials in metastatic colorectal cancer and pancreatic cancer (in which Hedgehog ligands are similarly overexpressed) involving the SMO antagonist vismodegib yielded negative results (Berlin et al., 2013; Catenacci et al., 2015). A better understanding of the interactions between Hedgehog and WNT signaling in colorectal cancer may therefore lead to the development of more effective therapies.

Here, using patient-derived 3D *in vitro* and xenograft models of colon cancer, we show that Hedgehog signaling in CSCs is non-canonical, SHH-dependent, and PTCH1-dependent and acts as a positive regulator of WNT signaling to regulate the survival of colon CSCs.

RESULTS

3D *In Vitro* Cancer Organoid Models and Xenografts of Colon Cancers Vary in CSC Frequency

Cancer organoid models were established from freshly isolated primary tumors and metastases from colon cancer patients (Table S1) by embedding in growth-factor reduced Matrigel (Figure 1A, top) and cultivating in serum-free medium (Sato et al., 2011; Schütte et al., 2017). To determine the frequency of tumor-initiating cells (TICs) in each model, cells were transplanted into immunocompromised mice at limiting dilution concentrations (Figure 1A). These results demonstrated a broad range of tumorigenic potential among patient models, ranging from 1 in 28,008 (95% confidence interval [CI], 1 in 7,039 to 1 in 111,406) at the lowest to 1 in 56 (95% CI, 1 in 20.6 to 1 in 151) at the highest. The TIC-enriched tumors had an enhanced growth rate compared with tumors with lower TIC frequencies (Figures 1B and 1C; Figure S1). In addition, the most TIC-enriched cancer organoids, 302-CB-M and 195-CB-P, were derived from high-grade stage IVA patient tumors (Figure 1A; Table S1). There was no correlation between major pathway mutations (*APC*, *TP53*, *KRAS*, *SMAD4*, and *PIK3CA*) (Table S2) or microsatellite instability, detected in 261-MB-P and 278-ML-P (Schütte et al., 2017), and differences in TIC capacity or growth rate.

The ability of CSCs to survive and form spheroids in non-adherent cell culture is the gold standard assay for the assessment of CSCs *in vitro* (Ricci-Vitiani et al., 2007; Weiswald et al., 2015). Therefore, to determine the frequency of CSCs in the cancer organoid models, seven models (281-CB-P, 261-MB-P, 162-MW-P, 151-ML-M, 278-ML-P, 302-CB-M, and 195-CB-P) were distributed by fluorescence-activated cell sorting (FACS) into low-attachment plates and assessed for spheroid formation (Figure 1D). These data showed that the frequency of *in vitro* CSCs in each cancer organoid model correlated with the frequency of TICs *in vivo* (Figure 1A) and demonstrate that cancer organoids are functionally heterogeneous and vary in CSC frequency.

CSC Frequency Correlates with Expression of Stem Cell-Associated Genes and Developmental Pathways

To investigate the molecular basis of the differential CSC frequencies, cancer organoid models were stained for the differentiation markers MUC2 and KRT20, the stem cell-associated WNT signaling protein BETA-CATENIN (Figure 2A; Figure S2A; Movies S1 and S2), and the structural protein F-ACTIN. MUC2 and KRT20 staining demonstrated the cancer organoids to be largely undifferentiated, and BETA-CATENIN was found to be strongly expressed in all models. However, differences in nuclear localization of BETA-CATENIN suggested varying levels of WNT signaling activity both within and between tumor models. The localization of F-ACTIN to the apical/luminal surface of the cancer organoids demonstrated that they retain the strong apical-basal polarity of the normal intestine.

RNA sequencing analysis demonstrated further molecular differences between the cancer organoids (Figure 2B). Analysis of stem cell-associated (*ALDH1A1*, *ASCL2*, *AXIN2*, *CTNNB1*, *EPHB2*, *LRIG1*, *OLFM4*, and *PHLDA1*) (Douville et al., 2009; Shenoy et al., 2012; Schuijers et al., 2015; Merlos-Suárez et al., 2011; Wong et al., 2012; van der Flier et al., 2009; Sakthianandeswaren et al., 2011; Huang et al., 2009), proliferation (*MKI67* and *MYC*), and differentiation (*ATOH1* and *MUC2*) (Yang et al., 2001; Shroyer et al., 2007) transcripts demonstrated higher stem cell gene expression in the more CSC-enriched tumors, which also had lower expression of the differentiation markers *ATOH1* and *MUC2*. These data were validated by RT-PCR gene expression analysis (Figure 2C).

To identify pathways that may regulate colon CSCs, gene set enrichment analysis (GSEA) was carried out, comparing CSC-enriched model 195-CB-P to model 162-MW-P, which had a 173-fold reduced TIC frequency compared with model 195-CB-P and failed to form spheroids at low cell number. These analyses demonstrated the transcriptome of 195-CB-P cells to be enriched for gene sets associated with development, including organ development and WNT signaling (Figure 2C; Figure S2). Interestingly, core enrichment analysis of WNT BETA-CATENIN signaling identified the Hedgehog signaling component and

A

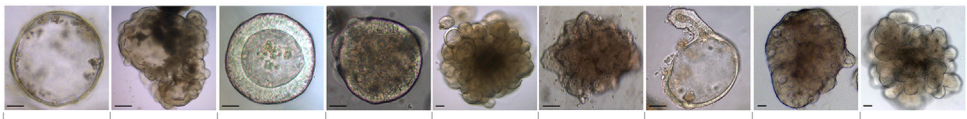

Cell Dilution	281-CB-P	261-MB-P	162-MW-P	159-MB-P	238-CB-P	151-ML-M	278-ML-P	302-CB-M	195-CB-P
100 cells	0/6	2/6	1/6	3/6	3/6	1/6	5/6	4/6	5/6
1,000 cells	0/6	0/6	1/6	3/6	1/6	4/6	5/6	6/6	6/6
10,000 cells	2/6	3/6	3/6	4/6	5/6	5/6	6/6	5/5	6/6
Frequency of Tumor Initiating Cells	1 in 28,008	1 in 9,798	1 in 9,702	1 in 3,677	1 in 3,329	1 in 2,650	1 in 248	1 in 91	1 in 56
(95% confidence limits)	(1 in 7,039 - 1 in 111,406)	(1 in 3,750 - 1 in 25,603)	(1 in 3,721 - 1 in 25,293)	(1 in 1,490 - 1 in 9,070)	(1 in 1,328 - 1 in 8,345)	(1 in 1,006 - 1 in 6,980)	(1 in 90- 1 in 686)	(1 in 32.5 - 1 in 254)	(1 in 20.6 - 1 in 151)
Tumor Stage at Surgical Resection	IIA	I	IIA	IIIB	IIA	IVA	IIB	IVA	IVA

B

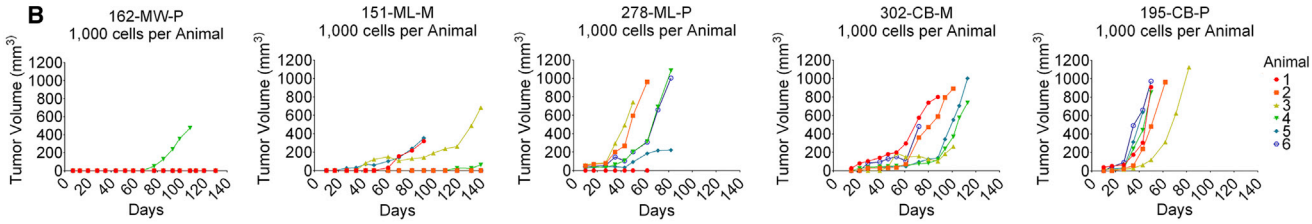

C

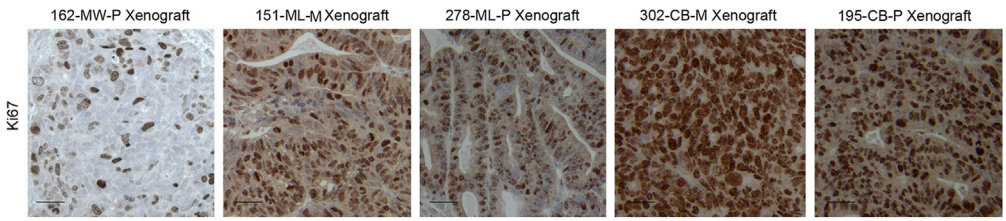

D

Cell dilution	281-CB-P	261-MB-P	162-MW-P	151-ML-M	278-ML-P	302-CB-M	195-CB-P
1 cell	0/64	0/64	0/64	2/64	2/64	6/64	5/64
10 cells	0/16	0/16	0/16	1/16	6/16	6/16	6/16
100 cells	0/16	4/16	0/16	15/16	16/16	16/16	16/16
Frequency of *in vitro* Sphere Forming Cells	NA	1 in 404	NA	1 in 45	1 in 21.8	1 in 15.4	1 in 16.8
(95% confidence limits)	NA	(1 in 152 - 1 in 1,071)	NA	(1 in 45 - 1 in 75.8)	(1 in 12.4 - 1 in 38.3)	(1 in 8.85- 1 in 26.9)	(1 in 9.55 - 1 in 29.4)

Figure 1. Tumor-Initiating CSCs in Patient-Derived Colon Cancer Organoids Vary in Frequency and Are Enriched in More Advanced Tumors

(A) Images of 3D cancer organoid models of patient-derived colon cancers (top; scale bars, 200 μm). The table shows results of limiting dilution transplantation of cells from each cancer organoid model as well as the staging of the original patient material (see also Tables S1 and S2). The number of established tumors as a fraction of the number of animals transplanted is given. Data are from five independent transplant sessions.

(B and C) Growth curves (B; see also Figure S1) and Ki67 staining (C) for five xenograft models. Scale bars, 20 μm.

(D) Results of the limiting dilution spheroid formation assay. The number of spheroids formed as a fraction of the number of cells seeded per well is given. Data are from two independent experiments.

target gene *PTCH1* to be differentially expressed in CSC-enriched 195-CB-P cells.

Hedgehog Signaling in CSC-Enriched Cancer Organoids Is Autocrine and GLI Independent

Hedgehog signaling has been shown to be a negative regulator of WNT signaling (van den Brink et al., 2004; Akiyoshi et al., 2006) and to be inactive in colon cancer cell lines (Chatel et al., 2007). It was therefore surprising to see enrichment for both WNT signaling genes and *PTCH1*, which is both the receptor for Hedgehog signals and a direct target gene, in the most CSC-enriched tumor model. To further investigate the role of Hedgehog signaling in CSCs, the expression of specific Hedgehog signaling genes was analyzed (Figure 3A and 3C). All models expressed the Hedgehog signaling genes *SHH*, *IHH*, and *SMO* as well as the direct signaling target *PTCH1* and downstream

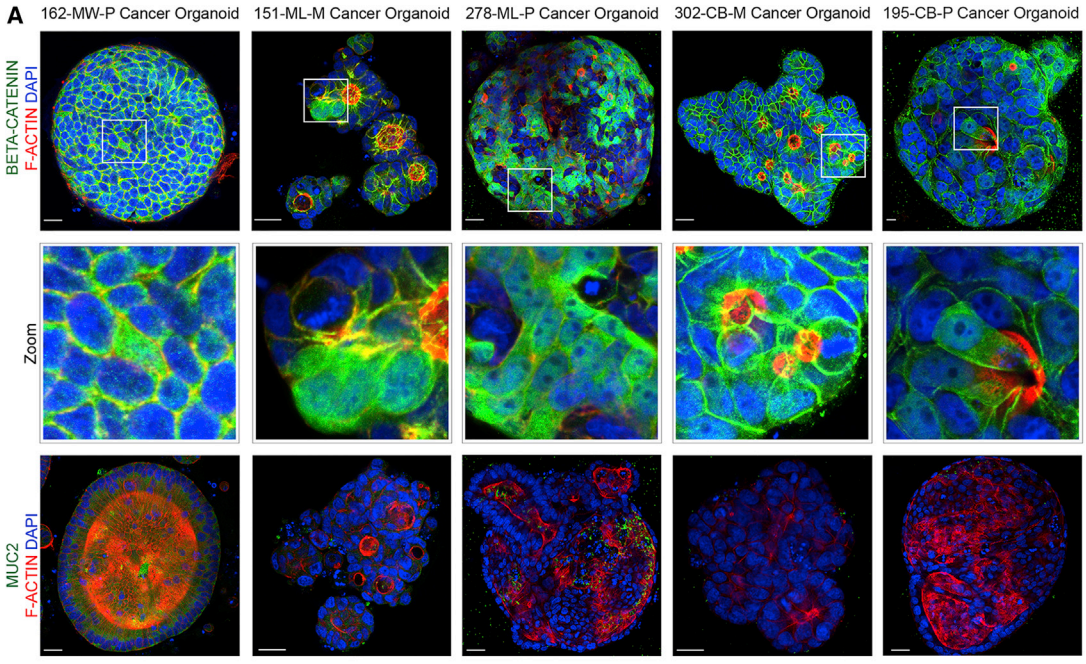

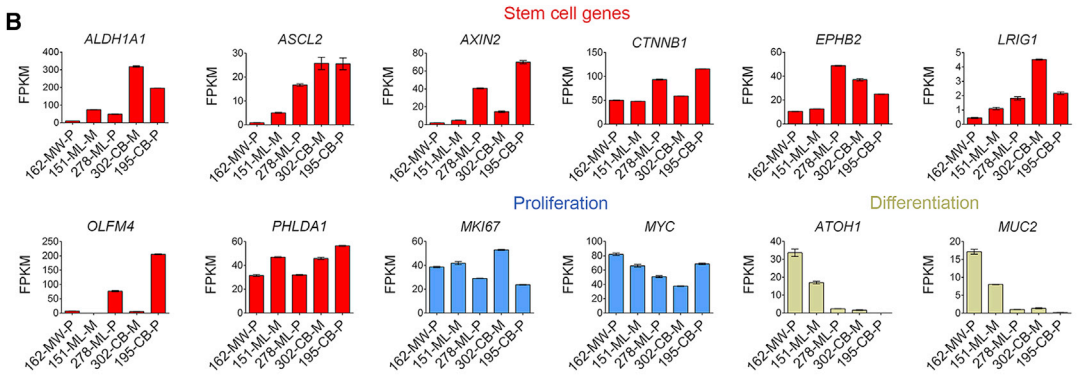

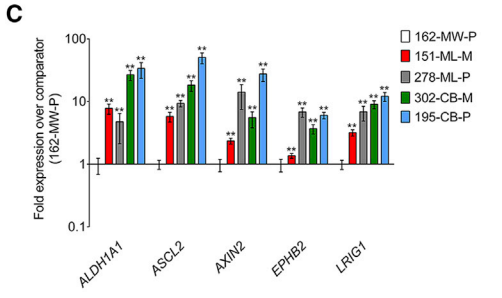

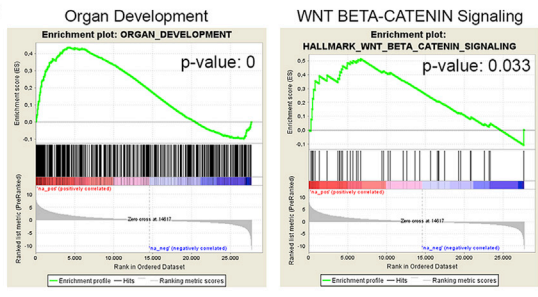

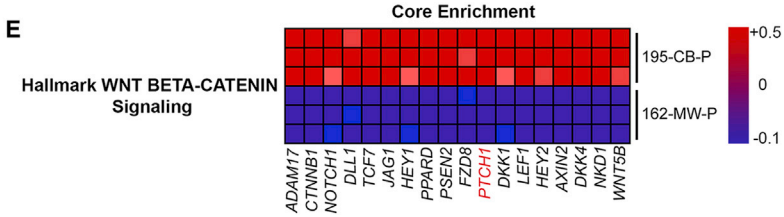

(legend on next page)

targets *BMP4*, *BMP7*, *BMI1*, *S100A4*, and *SOX9* (Yoshino et al., 2016; Roberts et al., 1995; Yoshimoto et al., 2012; Wang et al., 2012; Xu et al., 2014; Park et al., 2010; Figure 3A). There were no mutations detected in any Hedgehog signaling components that could lead to constitutive pathway activation (Schütte et al., 2017). Interestingly, the Hedgehog signaling targets tended to be more highly expressed in CSC-enriched models. Notably, expression of *GLI1*, *GLI2*, and *GLI3*, the effectors of canonical Hedgehog signaling, were markedly low (*GLI1*, 0.322–0.063 fragments per kilobase of transcript per million mapped reads [FPKM]; *GLI2*, 0.12–0.009 FPKM; *GLI3*, 0.608–0.004 FPKM). The minimum transcript level for functional expression of a gene is generally considered to be 1 FPKM (Vogel and Marcotte, 2012; Hebenstreit et al., 2011). These data, therefore, suggested that Hedgehog signaling is GLI-independent. To investigate this further, immunostaining of Hedgehog signaling proteins was carried out. Immunostaining of cancer organoids and corresponding xenografts for the Hedgehog signaling proteins SHH, SMO, PTCH1, and BMI1 further demonstrated Hedgehog signaling to be active in these tumors (Figure 3B; Figure S3). In addition, the ubiquitous expression of the Hedgehog ligand SHH and the target gene PTCH1 in all cells demonstrated that Hedgehog signaling in cancer organoids is autocrine. Concurring with the low transcript levels (< 1 FPKM), nuclear GLI1 protein was not detected by immunofluorescence staining in CSC-enriched cancer organoids (Figure 3B; Figure S3). However, it was detected in the CSC-depleted models 281-CB-P and 261-MB-P (Figure S3). Conversely, *in vivo*, where tumor cells are more differentiated than under the serum-free, undifferentiated conditions of the cancer organoid culture system, GLI1 was localized to the nucleus. However, immunostaining of frozen xenograft sections for GLI1 demonstrated that rare GLI1-negative cells also exist *in vivo* (Figure 3D; Figure S4). These data suggest that GLI-dependent Hedgehog signaling is required for the differentiation of tumor cells but that GLI-independent Hedgehog signaling, observed in CSC-enriched cancer organoids, may be important for maintaining CSCs in an undifferentiated state.

Colon Cancer Organoids Are Enriched for ALDH^{Positive} CSCs, in which Hedgehog Signaling Is GLI Independent

If the cancer organoids contain a subpopulation of CSCs, then it is possible that GLI transcripts were not detected in the RNA sequencing analysis of the unfractionated tumor cells. Increased aldehyde dehydrogenase (ALDH) activity, as measured using the Aldefluor assay, is a marker of CSC subpopulations in colon cancer and many other cancer types (Huang et al., 2009; Shenoy et al., 2012; Douville et al., 2009). ALDH^{Positive} and ALDH^{Negative} cells were therefore isolated (Figure 4A) to investigate differences in Hedgehog signaling components between cellular subpopulations. These data demonstrated that the cancer organoids are enriched for ALDH^{Positive} cells and that the frequency of ALDH^{Positive} cells is greatly decreased *in vivo* (Figure 4B). Limiting dilution serial xenotransplantation assays carried out with ALDH^{Positive} and ALDH^{Negative} cells confirmed that ALDH^{Positive} cells are enriched for CSCs (Figure 4C), which also tended to generate faster-growing tumors than ALDH^{Negative} cells (Figures 4D and 4E). RNA sequencing and GSEA of ALDH^{Positive} and ALDH^{Negative} cells isolated from cancer organoids demonstrated that ALDH^{Positive} CSCs are enriched for WNT and Hedgehog signaling transcripts but lack *GLI* (Figures 4F and 4G; Figure S5). Gene expression analysis of ALDH^{Positive} and ALDH^{Negative} xenograft cells also demonstrated that *in vivo* ALDH^{Positive} CSCs are enriched for stem cell (*ALDH1A1*, *BMI1*, and *EPHB2*), WNT (*AXIN2*, *CTNNB1*, and *LGR5*), and Hedgehog transcripts (*SHH*, *PTCH1*, and *BMP4*) but do not express *GLI1* (Figure 4H).

Non-canonical Hedgehog Signaling Is a Positive Regulator of WNT

WNT signaling pathway activation leads to the stabilization and nuclear translocation of BETA-CATENIN, which then complexes with the TCF/LEF transcription factors to activate WNT-responsive genes. Therefore, to further investigate the relationship between WNT and Hedgehog signaling in CSCs, WNT signaling reporter models were generated by transducing cells with a TCF/LEF-EGFP construct (Figure 5A). FACS analysis of TCF/LEF-EGFP cells demonstrated that WNT signaling activity positively correlated with the CSC frequency of the tumor models (Figures 5B and 5C). In addition, ALDH^{Positive} cells were enriched for TCF/LEF-EGFP^{Positive} cells, and this enrichment was also positively correlated with CSC frequency (Figure 5D). Gene expression analysis further demonstrated that TCF/LEF-EGFP^{Positive} cells were enriched for stem cell (*ALDH1A1* and *ASCL2*), WNT (*AXIN2*, *CTNNB1*, and *LGR5*), and Hedgehog (*SHH*, *SMO*, *PTCH1*, and *BMP4*) transcripts but not *GLI1* (Figure 5E).

To further delineate the role of GLI-independent Hedgehog signaling in colon CSCs and its relationship to WNT, cancer organoids were treated with small-molecule inhibitors of WNT signaling (the Tankyrase inhibitor NVP-TNKS656), SMO-dependent canonical Hedgehog signaling (the SMO inhibitors vismodegib and cyclopamine), and SHH signaling (the Hedgehog acyltransferase [HHAT] inhibitor RU-SKI 43). HHAT-mediated palmitoylation of SHH is required for SHH signaling (Chen et al., 2004). HHAT inhibition therefore blocks all signaling downstream of SHH, including non-canonical SMO-independent PTCH1-dependent Hedgehog signaling. Inhibition of Tankyrase

Figure 2. CSC-Enriched Cancer Organoids Are Poorly Differentiated and Are Enriched for WNT and Hedgehog Signaling

(A) Immunofluorescence staining of cancer organoids for BETA-CATENIN (green) (top), with magnified regions showing nuclear BETA-CATENIN (center), MUC2 (green) (bottom), and F-ACTIN (red). Nuclei are stained blue with DAPI (scale bars, 20 μm) (see also Movies S1 and S2).

(B) RNA sequencing-generated FPKM values from four different biological replicates for stem cell (red), proliferation (blue), and differentiation (beige) genes.

(C) RT-PCR validation of stem cell genes (fold expression ± 95% CIs) from three different biological replicates (see also Table S4). Significant differences are as follows: *$p < 0.05$, **$p < 0.01$.

(D) GSEA for organ development (nominal $p = 0$) and WNT signaling (nominal $p = 0.033$) in CSC-enriched 195-CB-P cancer organoids compared with CSC-low 162-MW-P cancer organoids ($n = 3$ separate cell preparations).

(E) Heatmap showing core enrichment hallmark WNT BETA-CATENIN signaling genes in 195-CB-P cells compared with 162-MW-P cells (see also Figure S2).

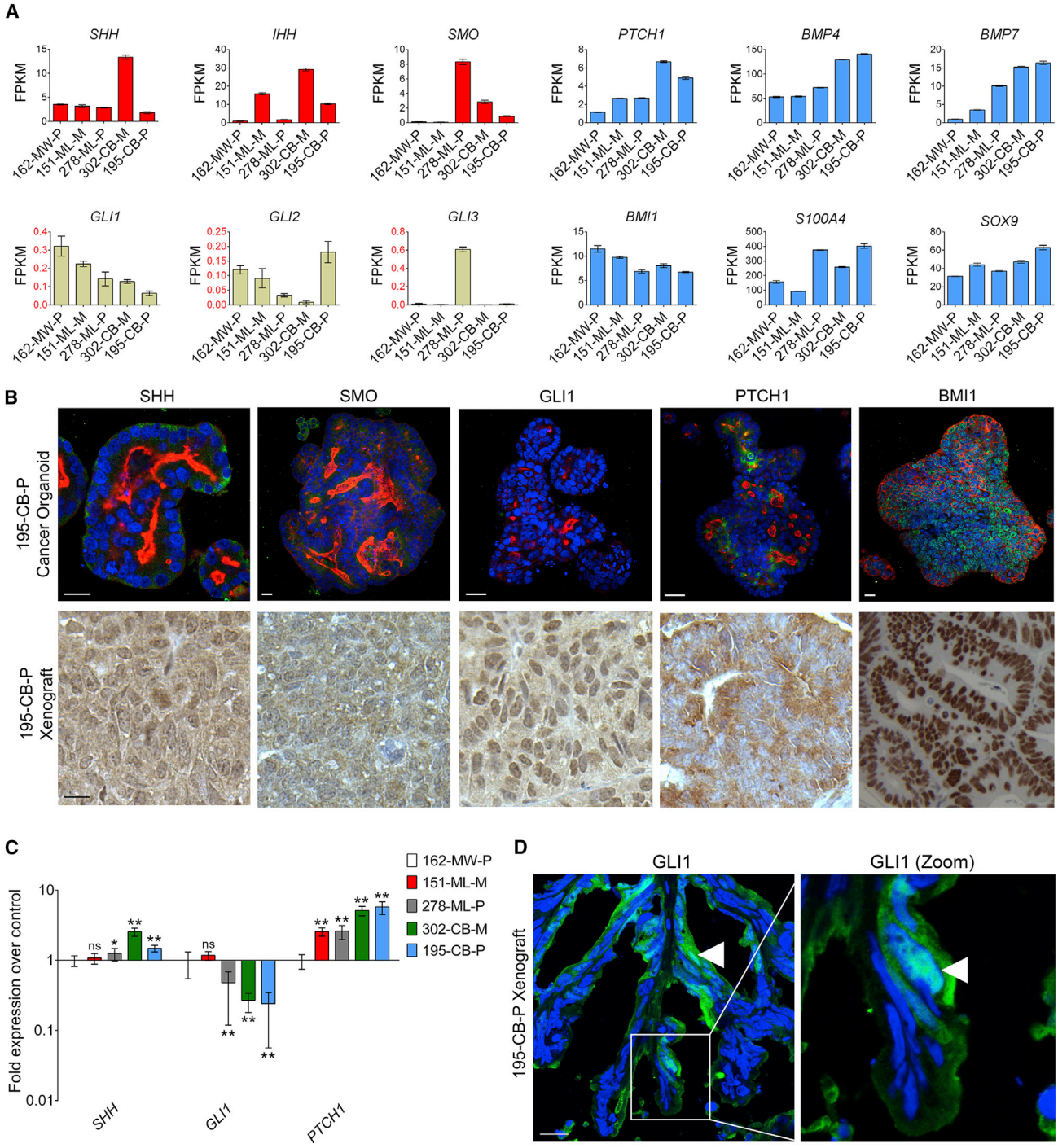

Figure 3. Hedgehog Signaling in Colon CSCs Is Autocrine and GLI Independent

(A) RNA sequencing-generated FPKM values for Hedgehog signaling genes. FPKM values for *GLI1*, *GLI2*, and *GLI3* (red) were less than 1 FPKM (n = 3 separate cell preparations).

(B) Immunofluorescence staining (top) of 195-CB-P cancer organoids for the Hedgehog signaling proteins SHH, SMO, GLI1, PTCH1, BMI1 (green), and F-ACTIN (red) (see also Figure S3). Nuclei are stained blue with DAPI (scale bars, 20 μm). Also shown is immunohistochemistry (bottom) of 195-CB-P xenografts for SHH, SMO, GLI1, PTCH1 and BMI1 (scale bars, 20 μm).

(C) RT-PCR validation of Hedgehog genes (fold expression ± 95% CIs) from three different biological replicates (see also Table S4). Significant differences are as follows: *$p < 0.05$, **$p < 0.01$.

(D) Immunofluorescence staining for GLI1 (green) in a frozen 195-CB-P xenograft section (scale bar, 20 μm). Arrowheads indicate nuclear GLI1 staining. The box contains cells lacking nuclear GLI1 staining (see also Figure S4).

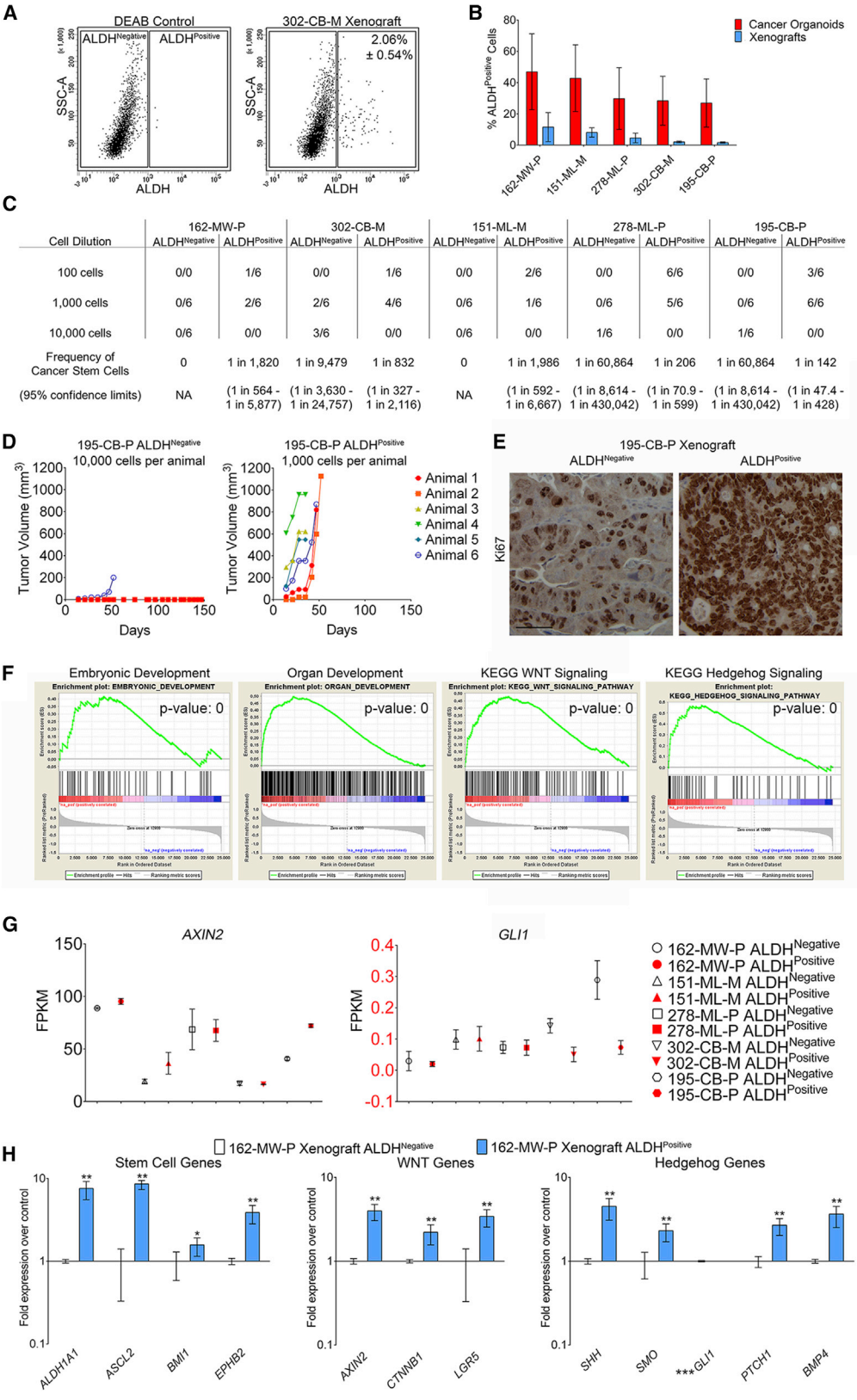

(legend on next page)

and SMO-dependent canonical Hedgehog signaling had no effect on cell survival at low doses (half maximal inhibitory concentration [IC_{50}] values > 10 μM) (Figure 5F). However, RU-SKI 43 effectively reduced cell survival at low doses in all models (IC_{50} values < 10 μM). Significantly, addition of recombinant SHH to the culture medium blocked the effect of RU-SKI 43 (Figure 5G). These data further demonstrate that Hedgehog signaling is active in colon CSCs and suggest that CSCs are dependent on SMO-independent, PTCH1-dependent, non-canonical Hedgehog signaling for survival.

To determine the effect of Hedgehog signaling pathway inhibition on WNT activity, 151-ML-M TCF/LEF-EGFP cells were treated with either vismodegib or RU-SKI 43 prior to FACS analysis to determine the effect on WNT activity based on changes in GFP. Interestingly, inhibiting SMO-dependent canonical Hedgehog signaling with vismodegib led to an increase in TCF/LEF-$EGFP^{Positive}$ cells (Figures 5H and 5I). However, targeting SHH signaling upstream of SMO and PTCH1 using RU-SKI 43 significantly decreased WNT activity. These data support previous reports that canonical Hedgehog signaling is a negative regulator of WNT activity (van den Brink et al., 2004) and suggest that non-canonical Hedgehog signaling is a positive regulator of WNT.

Non-canonical PTCH1-Dependent Hedgehog Signaling Is Required for the Survival of Colon CSCs

To determine whether non-canonical Hedgehog signaling is functionally required for the survival of CSCs, cells were transduced in non-adherent culture with three different lentiviral short hairpin RNAs (shRNAs) against *HHAT* (shRNA HHAT 1, shRNA HHAT 2, and shRNA HHAT 3). Successful knockdown of *HHAT* was confirmed by qRT-PCR (Figures 6A and 7D). With the exception of 278-ML-P and 195-CB-P (shRNA HHAT2), shRNAs against *HHAT* had little effect on the proliferation of cancer organoid models in Matrigel culture (Figure S6).

To determine whether non-canonical Hedgehog signaling is required for CSC survival and proliferation in non-adherent culture, $GFP^{Positive}$ shRNA HHAT cells were sorted by FACS into ultra-low attachment plates. In all models, shRNA HHAT led to a significant decrease in the frequency of spheroid formation (Figure 6B). The shRNA HHAT spheroids that did form were significantly smaller than control transduced cells (Figures 6C and 6D). Addition of recombinant SHH to the culture medium attenuated the effect of shRNA HHAT on sphere formation (Figure 6E). These data demonstrate that non-canonical Hedgehog signaling is required for CSC survival and that it requires SHH. In addition, these data suggest that the variance in effect on proliferation between RU-SKI 43 (Figure 5F) and shRNA HHAT in adherent cells (Figure S6) may be due to the preferential loss of more HHAT-dependent cells during transduction in non-adherent culture, leading to a mitigation of the effect on proliferation of cells in adherent culture.

To investigate which of the HHAT downstream Hedgehog signaling components is required for CSC survival, cells were transfected with small interfering RNAs (siRNAs) against *SMO* and *PTCH1* (Figure S6). siRNA PTCH1 caused a significant decrease in spheroid formation in all models (Figure 6F). However, similar to treatment with SMO inhibitors, siRNAs against *SMO* had no effect on survival. Taken together, these data demonstrate that colon CSC survival is PTCH1-dependent.

Non-canonical Hedgehog Signaling Regulates the Frequency of Colon CSCs

Having demonstrated that non-canonical Hedgehog signaling is required for the survival of CSCs, we carried out gene expression analysis on shRNA HHAT cancer organoids to investigate the effect on stem cell, WNT, and Hedgehog signaling genes (Figure 6G). *HHAT* knockdown caused a decrease in expression of the WNT signaling genes *AXIN2*, *CTNNB1*, and *RUNX2* as well as the Hedgehog signaling genes *SHH*, *SMO*, and *PTCH1*. Of these, *AXIN2* and *PTCH1*, key WNT and Hedgehog target genes (Wu et al., 2012; Ingham, 1998; Marigo and Tabin, 1996; You et al., 2010), were most significantly downregulated. The decreased expression of *CTNNB1*, which is not a direct target of WNT, is most likely due to the loss of *CTNNB1*-expressing cells rather than downregulation of its expression. The stem cell-associated genes *ALDH1A1*, *ASCL2*, *BMI1*, and *EPHB2* (Merlos-Suárez et al., 2011; Douville et al., 2009; Huang et al., 2009; Kreso et al., 2014) also decreased in expression, and of these, *ASCL2*, the WNT-responsive master regulator of intestinal stem cell fate (Schuijers et al., 2015), was most significantly affected by shRNA HHAT. In addition, FACS analysis of control virus-transduced and shRNA HHAT-transduced cells for ALDH activity demonstrated a decrease in the frequency of

Figure 4. Colon Cancer Organoids Are Enriched for $ALDH^{Positive}$ CSCs that Lack GLI

(A) Representative Aldefluor assay FACS plots of xenografts derived from cancer organoid model 302-CB-M (data are from 10 independent experiments). DEAB (diethylaminobenzaldehyde) is a specific inhibitor of ALDH and is used to control for background fluorescence.

(B) Frequency (± SD) of $ALDH^{Positive}$ cells in cancer organoids and corresponding xenografts (data are from 10 independent experiments, except for 162-MW-P xenografts, which were analyzed in three independent experiments).

(C) The table shows results of limiting dilution serial xenotransplantation of $ALDH^{Positive}$ and $ALDH^{Negative}$ cells from previously established cancer organoid-derived xenograft models. The number of successfully established tumors as a fraction of the number of animals transplanted is given. Data are from three independent transplant sessions. The p values for pairwise tests of differences in CSC frequencies between $ALDH^{Positive}$ versus $ALDH^{Negative}$ cells in 162-MW-P, 151-ML-M, 278-ML-P, 302-CB-M, and 195-CB-P tumors are 8.75×10^{-5}, 6.47×10^{-4}, 1.12×10^{-4}, 8.02×10^{-15}, and 4.72×10^{-13}, respectively.

(D and E) Growth curves (D) and Ki67 staining (E) for 10,000 195-CB-P $ALDH^{Negative}$ cells and 1,000 195-CB-P $ALDH^{Positive}$ cells (scale bar, 20 μm).

(F) GSEA for embryonic development (nominal p = 0), organ development (nominal p = 0), WNT (nominal p = 0), and Hedgehog signaling (nominal p = 0) in $ALDH^{Positive}$ cells (compared with $ALDH^{Negative}$ cells) from cancer organoid models 162-MW-P, 151-ML-M, 278-ML-P, 302-CB-M, and 195-CB-P (n = 3 separate cell preparations).

(G) RNA sequencing-generated FPKM values for *AXIN2* and *GLI1* in $ALDH^{Positive}$ and $ALDH^{Negative}$ cells (see also Figure S5).

(H) Fold expression of stem cell, WNT, and Hedgehog gene expression data ± 95% CIs in 162-MW-P $ALDH^{Positive}$ xenograft cells compared with 162-MW-P $ALDH^{Negative}$ xenograft cells (see also Table S4). ***, *GLI1* expression was below the limits of detection. Significant differences are as follows: *p < 0.05, **p < 0.01.

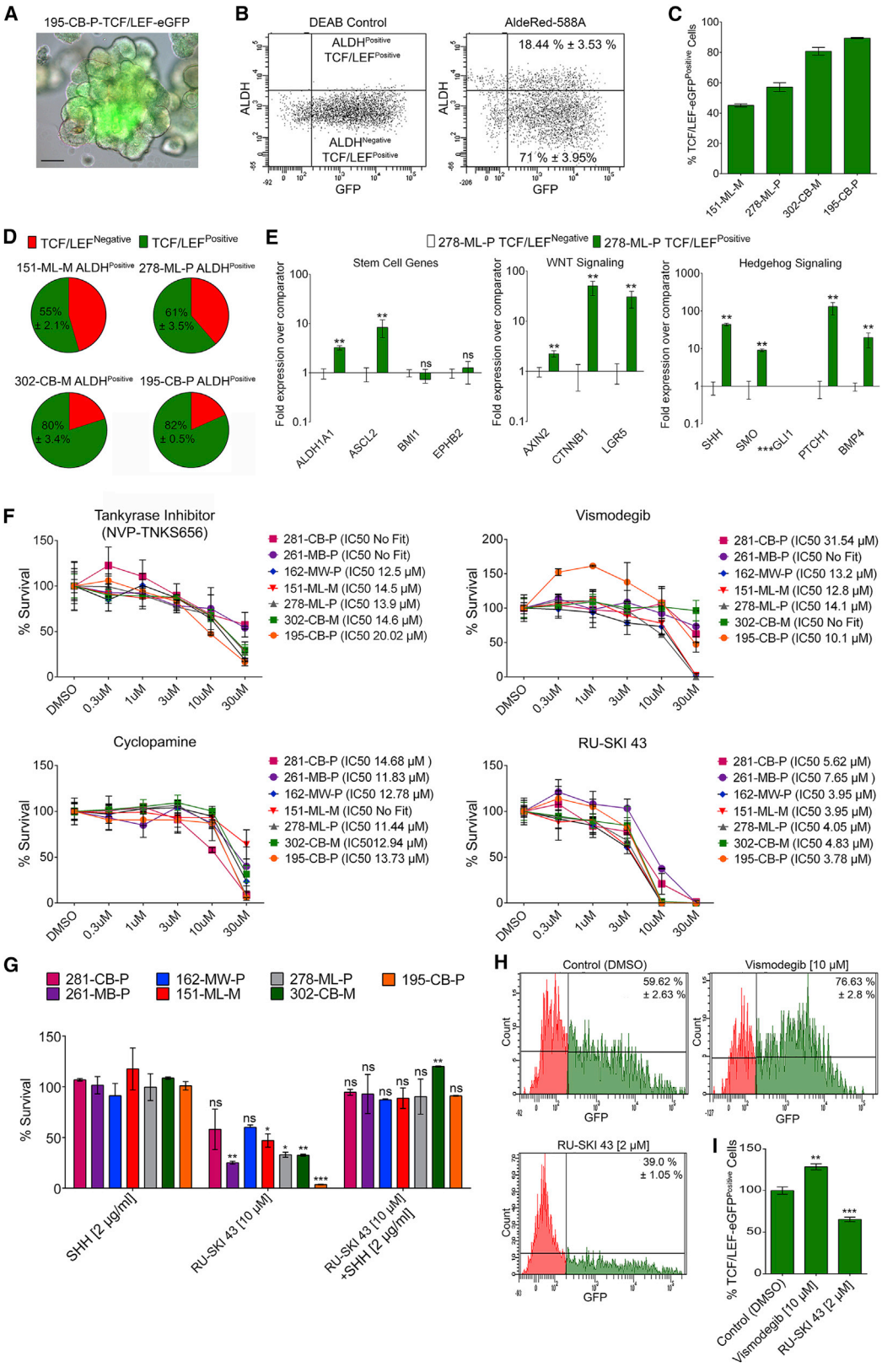

(legend on next page)

ALDH^{Positive} cells in shRNA HHAT cancer organoids (Figures 6H and 6I). These data demonstrate that non-canonical Hedgehog signaling regulates the frequency of CSCs in colon cancer.

Non-canonical Hedgehog Signaling Regulates WNT Signaling and the Differentiation of CSCs *In Vivo*

Limiting dilution xenotransplantation of control virus-transduced and shRNA HHAT-transduced high-grade IVA 195-CB-P and low-grade IIB 278-ML-P cells were carried out to determine whether non-canonical Hedgehog signaling regulates tumorigenesis *in vivo*. Control virus-transduced cells generated xenografts at each cell dilution tested, but shRNA HHAT-transduced cells were significantly impaired in their ability to generate tumors when transplanted at low cell numbers (Figure 7A). These data demonstrate that impairment of non-canonical Hedgehog signaling in CSCs significantly decreased their tumorigenic capacity. Immunohistochemistry of the shRNA HHAT tumor tissue demonstrated increased lumen formation compared with control tissue (Figure 7B), which, along with the slower growth rate (Figure 7C), suggested that the shRNA HHAT tumors were more differentiated, although there was no increase in staining for the differentiation markers KRT20 or MUC1 (data not shown). qRT-PCR analysis of three of the shRNA HHAT tumors confirmed that shRNA HHAT knockdown was present (Figure 7D). Significantly, WNT signaling gene expression was also found to be decreased. Conversely, the expression of differentiation markers, including the tumor suppressor and WNT target *ATOH1* (Bossuyt et al., 2009; Aragaki et al., 2008), was strongly increased. These data demonstrate that non-canonical Hedgehog signaling is a positive regulator of WNT signaling and is required to prevent the differentiation of CSCs *in vivo*.

PTCH1 Expression Correlates with Stem Cell Genes and WNT Signaling in Clinical Samples and Is Increased in Late-Stage Colorectal Cancers

Gene expression data demonstrated *PTCH1* to be enriched in CSC-enhanced cancer organoid models and in ALDH^{Positive} CSCs and TCF/LEF^{Positive} cellular subpopulations. To determine whether *PTCH1* is similarly expressed in patients, we carried out a pairwise correlation comparing the Hedgehog genes *SHH*, *PTCH1*, and *GLI1* with the stem cell genes *EPHB2* and *ASCL2*, the WNT genes *LGR5* and *AXIN2*, and the differentiation genes *ATOH1* and *MUC1* (Figure 7E). These data demonstrated that *PTCH1* expression is positively correlated with stem cell and WNT signaling genes and negatively correlated with differentiated genes in clinical samples. Significantly, *GLI1* expression was negatively correlated with both stem cell and WNT signaling genes.

To further characterize Hedgehog signaling in clinical samples, we carried out immunostaining of colorectal cancer tissue microarrays (Figure 7G; Figure S7). SHH and GLI1 were found to be ubiquitously expressed in epithelial cells and in the stroma, demonstrating that both paracrine and autocrine signaling takes place *in vivo*. These data support previous studies showing SHH to be ubiquitously expressed and required for the growth of colorectal tumors (Berman et al., 2003; Yoshikawa et al., 2009; Oniscu et al., 2004). PTCH1 staining was generally absent or weak. However, when PTCH1 staining was strong, it positively correlated with strong cytoplasmic and nuclear BETA-CATENIN in serially stained sections.

Analysis of *PTCH1* expression across different colon tumor stages demonstrated that *PTCH1* expression is more enhanced in late stage T4 clinical tumors compared with early T1 tumors (Figure 7F). Overall, these data suggest that *PTCH1* expression may be an indicator of poor prognosis in colorectal cancer.

DISCUSSION

Colon cancer organoids demonstrated both functional and molecular inter- and intratumor heterogeneity, with only a subpopulation of cells within each tumor being tumorigenic. The preserved functional heterogeneity observed within the cancer organoids strongly supports their validity as models for the delineation of signaling pathways important in the regulation of CSCs and tumor biology in general (van de Wetering et al., 2015; Clevers, 2016; Dutta et al., 2017).

The requirement of WNT signaling for the survival of normal and cancer stem cells is well established (Krausova and Korinek, 2014; Nusse, 2008; Kanwar et al., 2010; Vermeulen et al., 2010; Sato et al., 2011). Here we demonstrate that colon cancer organoids are enriched for ALDH^{Positive}, WNT-active TCF/LEF-EGFP^{Positive} CSCs and that WNT activity increases with CSC content. Canonical GLI-dependent Hedgehog signaling has been shown to be a negative regulator of WNT signaling both in the normal intestine, where is acts to restrict expansion of the stem cell compartment, and in colon cancer (van den Brink et al., 2004; Van Dop et al., 2009; Madison et al., 2005; Akiyoshi et al., 2006). It was therefore interesting that ALDH^{Positive} CSCs

Figure 5. Non-canonical Hedgehog Signaling Is a Positive Regulator of WNT Signaling in Colon Cancer

(A) Image of the 195-ML-P-TCF/LEF-EGFP reporter organoid (scale bar, 200 μm).

(B) Representative Aldefluor assay FACS plots of 195-ML-P-TCF/LEF-EGFP cells.

(C and D) Frequency (± SD) of TCF/LEF-EGFP^{Positive} cells in cancer organoid models (C, n = 2 independent experiments) and frequency of ALDH^{Positive} cells in TCF/LEF-EGFP$^{Positive\ and}$ TCF/LEF-EGFP^{Negative} subpopulations (D, n = 2 independent experiments).

(E) Fold expression of stem cell, WNT, and Hedgehog gene expression data ± 95% CIs in 278-ML-P TCF/LEF-EGFP^{Positive} cells compared with 278-ML-P TCF/LEF-EGFP^{Negative} cells (see also Table S4). ***, *GLI1* expression was below the limits of detection in these samples. Significant differences are as follows: *$p < 0.05$, **$p < 0.01$.

(F) Survival of cancer organoid models after 72 hr treatment with the Tankyrase inhibitor NVP-TNKS656, the SMO inhibitors vismodegib and cyclopamine, and the HHAT (SHH signaling) inhibitor RU-SKI 43. Data are from two independent experiments (± SD).

(G) Percent survival of cancer organoids after treatment with recombinant SHH, RU-SKI 43, or RU-SKI 43 in combination with 2 μg/mL recombinant SHH compared with untreated control.

(H and I) FACS plots (H) and frequency (I) of TCF/LEF-EGFP^{Positive} cells in 151-ML-M-WNT-EGFP organoids treated with DMSO, vismodegib (10 μM), or RU-SKI 43 (2 μM) for 24 hr (mean ± SD; data are from two independent experiments). *$p < 0.05$, **$p < 0.01$, ***$p < 0.001$ (t test).

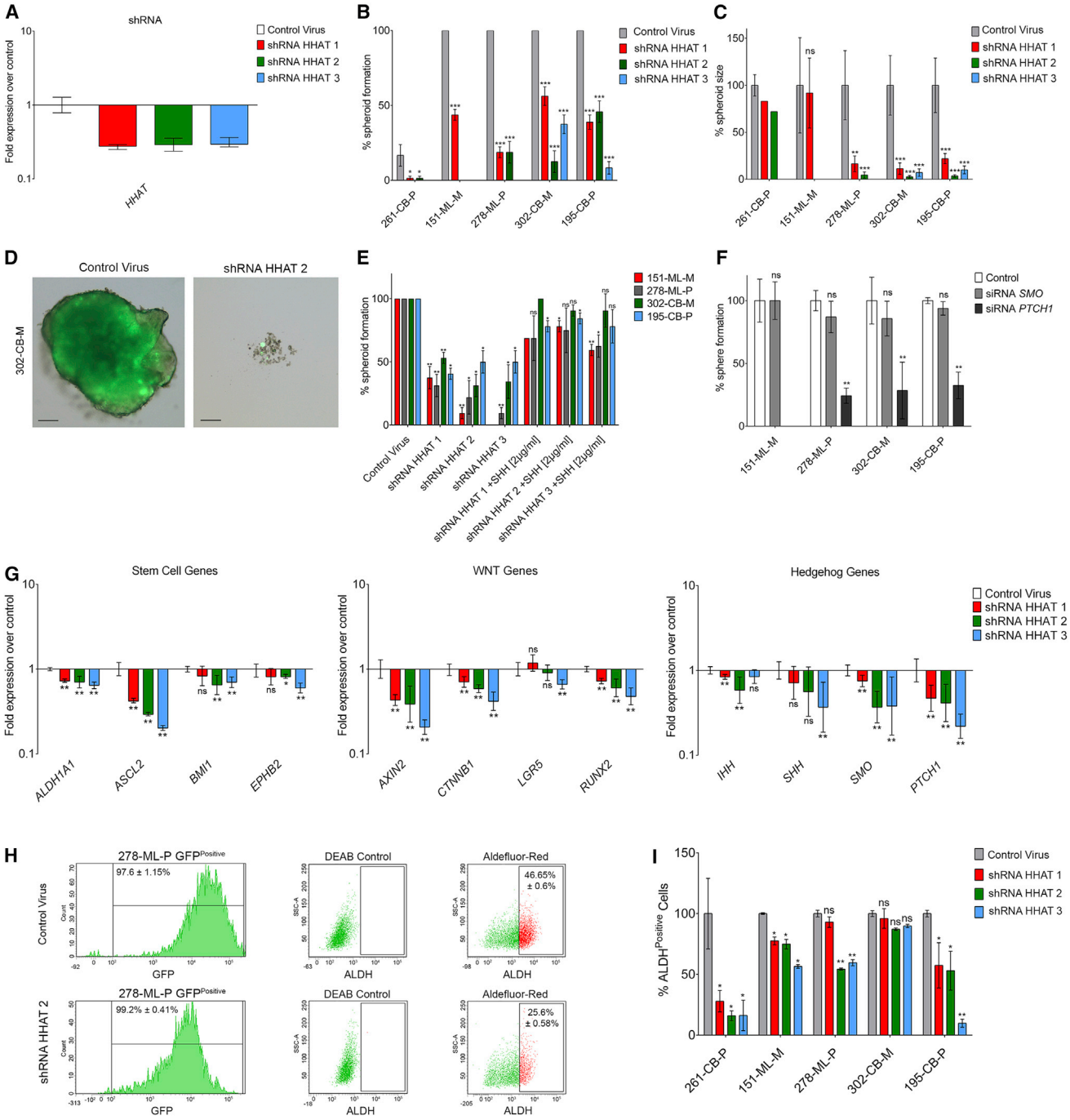

Figure 6. Non-canonical PTCH1-Dependent Hedgehog Signaling Regulates ALDH^{Positive} CSC Frequency and Is Required for the Survival of Colon CSCs in Non-adherent Cell Culture

(A) Fold expression of *HHAT* RT-PCR gene expression data ± 95% CIs in 151-ML-M cancer organoid cells transduced with three different shRNA HHAT-GFP lentiviruses (n = 3 independent cell preparations) over the comparator population (control virus transduced 151-ML-M cells) (see also Table S4).

(B) Frequency of shRNA HHAT spheroid formation in non-adherent cell culture compared with control-transduced cells (mean ± SD; data are from three independent experiments). *p < 0.05, ***p < 0.001 (t test) (see also Figure S6).

(C) shRNA HHAT spheroid size relative to control-transduced cells (mean ± SD; data are from three independent experiments). ns, not significant. **p < 0.01, ***p < 0.001 (t test).

(D) Representative images of a 302-CB-M control-GFP spheroid (left) and shRNA HHAT cells that did not form a spheroid (right) in non-adherent cell culture (scale bars, 100 µm).

(legend continued on next page)

and TCF/LEF-EGFP^{Positive} cells were enriched for both WNT and Hedgehog genes but lacked expression of *GLI*. In addition, targeting SHH with the HHAT inhibitor RU-SKI 43 and shRNA HHAT caused a decrease in WNT activity and decreased expression of stem cell, WNT, and Hedgehog signaling genes. Given that cancer organoid models are maintained in an undifferentiated state (high ALDH^{Positive} TCF/LEF-EGFP^{Positive} cell frequencies, MUC2-negative, KRT20-negative, GLI1-negative), with no differentiation factors in the culture medium, and that the *in vivo* environment promotes differentiation (low ALDH^{Positive} cell frequency, MUC2-positive, KRT20-positive, GLI1-positive), these data support a model wherein non-canonical Hedgehog signaling blocks differentiation and is a positive regulator of WNT.

Treatment of cancer organoids with small-molecule inhibitors and RNAi against the Hedgehog signaling components HHAT, SHH, SMO, and PTCH1 demonstrated that non-canonical Hedgehog signaling is required for CSC survival and is PTCH1-dependent and SMO-independent (type I non-canonical Hedgehog signaling). PTCH1 has been shown to function as a dependence receptor by inducing apoptosis in the absence of SHH ligand (Thibert et al., 2003; Mille et al., 2009; Mehlen and Bredesen, 2004). However, because siRNA PTCH1 also blocked sphere formation in non-adherent cell culture, it is unlikely that the effect on survival caused by loss of SHH through RU-SKI 43 or shRNA HHAT was due to PTCH1 acting as a dependence receptor.

SHH was ubiquitously expressed in cancer organoids and in epithelial and stromal cells *in vivo*, and the addition of recombinant SHH to RU-SKI 43-treated cancer organoids and shRNA HHAT spheroids attenuated the effect on survival. These data demonstrate that non-canonical Hedgehog signaling in cancer organoids is autocrine but that both paracrine (epithelium to mesenchyme) and autocrine signaling are active *in vivo* and support previous studies showing SHH to be ubiquitously expressed and required for tumor growth (Berman et al., 2003; Yoshikawa et al., 2009; Oniscu et al., 2004). In addition, *PTCH1* expression was found to be enriched both in CSCs and in late-stage T4 colorectal tumors and to positively correlate with stem cell genes and WNT signaling activity in clinical tumor samples. These data support *PTCH1* as a potential biomarker for colorectal cancer prognosis.

Based on these data, we propose a model wherein non-canonical PTCH1-dependent Hedgehog signaling acts as a positive regulator of WNT to maintain CSCs in an undifferentiated state, whereas canonical SMO-dependent Hedgehog signaling, mediated by nuclear localization of GLI1, leads to a downregulation of WNT signaling and tumor cell differentiation. Inducing CSC differentiation by targeting non-canonical Hedgehog signaling may therefore provide strategies for the elimination of therapy-resistant CSCs; for example, blocking SHH signaling by targeting HHAT in combination with standard-of-care tumor debulking therapies. Indeed, targeting of HHAT has also been proposed to have therapeutic potential for Hedgehog-dependent pancreatic cancer and breast cancers (Petrova et al., 2015; Matevossian and Resh, 2015).

These data demonstrate that SHH-dependent, PTCH1-dependent, non-canonical Hedgehog signaling is required for the survival of colon CSCs and support HHAT as a possible therapeutic target for the future development of anti-tumor treatments.

EXPERIMENTAL PROCEDURES

Human Tissue Samples and Establishment of Patient-Derived Cancer Organoid Cell Cultures

Tumor material was obtained with informed consent from colorectal cancer patients under approval from the local Institutional Review Board of Charité University Medicine (Charité Ethics, Charitéplatz 1, 10117 Berlin, Germany) (EA 1/069/11) and the ethics committee of the Medical University of Graz (Ethics Commission of the Medical University of Graz, Auenbruggerplatz 2, 8036 Graz, Austria), confirmed by the ethics committee of the St John of God Hospital Graz (23-015 ex 10/11). Tumor staging was carried out by experienced and board-certified pathologists (Table S1). Cancer organoid cultures were established and propagated as described by Schütte et al. (2017).

Limiting Dilution Xenotransplantation

Housing and handling of animals were in compliance with the European and German Guidelines for Laboratory Animal Welfare. Animal experiments were conducted in accordance with animal welfare laws, approved by local authorities, and in accordance with the ethical guidelines of Bayer. Cancer organoids were processed to single cells, and live cells were then injected subcutaneously in PBS and Matrigel (1:1 ratio) at limiting cell dilutions into female 8- to 10-week-old nude$^{-/-}$ mice. For serial xenotransplantation studies, tumors derived from limiting dilution transplants were processed to single cells and sorted by FACS (BD FACS Aria II) for ALDH activity (Aldefluor assay) and DAPI to exclude dead cells. Cells were then re-transplanted at limiting dilutions.

Statistical Analysis

GraphPad Prism 6.0 was used for data analysis and imaging. All data are presented as the means ± SD, followed by determining significant differences using two-tailed t test. The significance of RT-PCR data was determined by inspection of error bars as described by Cumming et al. (2007). Limiting dilution frequency and probability estimates were analyzed by the single-hit Poisson model and pairwise tests for differences in stem cell frequencies using the ELDA software (http://bioinf.wehi.edu.au/software/elda/index.html; Hu and Smyth, 2009). GSEA was carried out using the preranked feature of the Broad Institute GSEA software version 2 using msigdb v5.1 gene sets (Subramanian et al., 2005; Mootha et al., 2003). The ranking list was derived from the fold changes calculated from the differential gene expression calculation

(E) Frequency of shRNA HHAT spheroid formation in non-adherent cell culture in combination with recombinant SHH compared with control-transduced cells (mean ± SD; data are from two independent experiments). *p < 0.05, **p < 0.01 (t test).
(F) Frequency of siRNA SMO and siRNA PTCH1 spheroid formation in non-adherent cell culture compared with control-transfected cells (mean ± SD; data are from three independent experiments). *p < 0.05, **p < 0.01 (t test) (see also Figure S6).
(G) Fold expression of stem cell, WNT, and Hedgehog gene expression data ± 95% CIs in 151-ML-M cancer organoid cells transduced with three different shRNA HHAT lentiviruses (n = 3 independent cell preparations) compared with control virus-transduced 151-ML-M cells (see also Table S4). Significant differences are as follows: *p < 0.05, **p < 0.01.
(H and I) Representative Aldefluor assay FACS plots (H) and frequency (I) of ALDH^{Positive} cells in shRNA HHAT cells compared with control virus-transduced cells (mean ± SD; data are from two independent experiments). *p < 0.05, **p < 0.01, ***p < 0.001 (t test).

A

Cell Dilution	195-CB-P Control Virus	195-CB-P shRNA HHAT 1	195-CB-P shRNA HHAT 2	195-CB-P shRNA HHAT 3	278-ML-P Control Virus	278-ML-P shRNA HHAT 1	278-ML-P shRNA HHAT 2	278-ML-P shRNA HHAT 3
100 cells	3/5	0/5	0/5	0/5	5/5	0/5	1/5	3/5
1,000 cells	5/5	0/5	0/5	1/5	5/5	3/5	4/5	2/5
10,000 cells	5/5	0/5	4/5	3/5	5/5	4/5	5/5	5/5
Frequency of Tumor Initiating Cells	1 in 106	NA	1 in 7,840	1 in 9,341	1 in 1	1 in 3,692	1 in 580	1 in 830
(95% confidence limits)	(1 in 34.1 - 1 in 348)	NA	(1 in 2,874 - 1 in 21,388)	(1 in 3,301- 1 in 26,436)	(1 in 1 - 1 in 125)	(1 in 1,374 - 1 in 9,921)	(1 in 218- 1 in 1,543)	(1 in 299- 1 in 2,307)

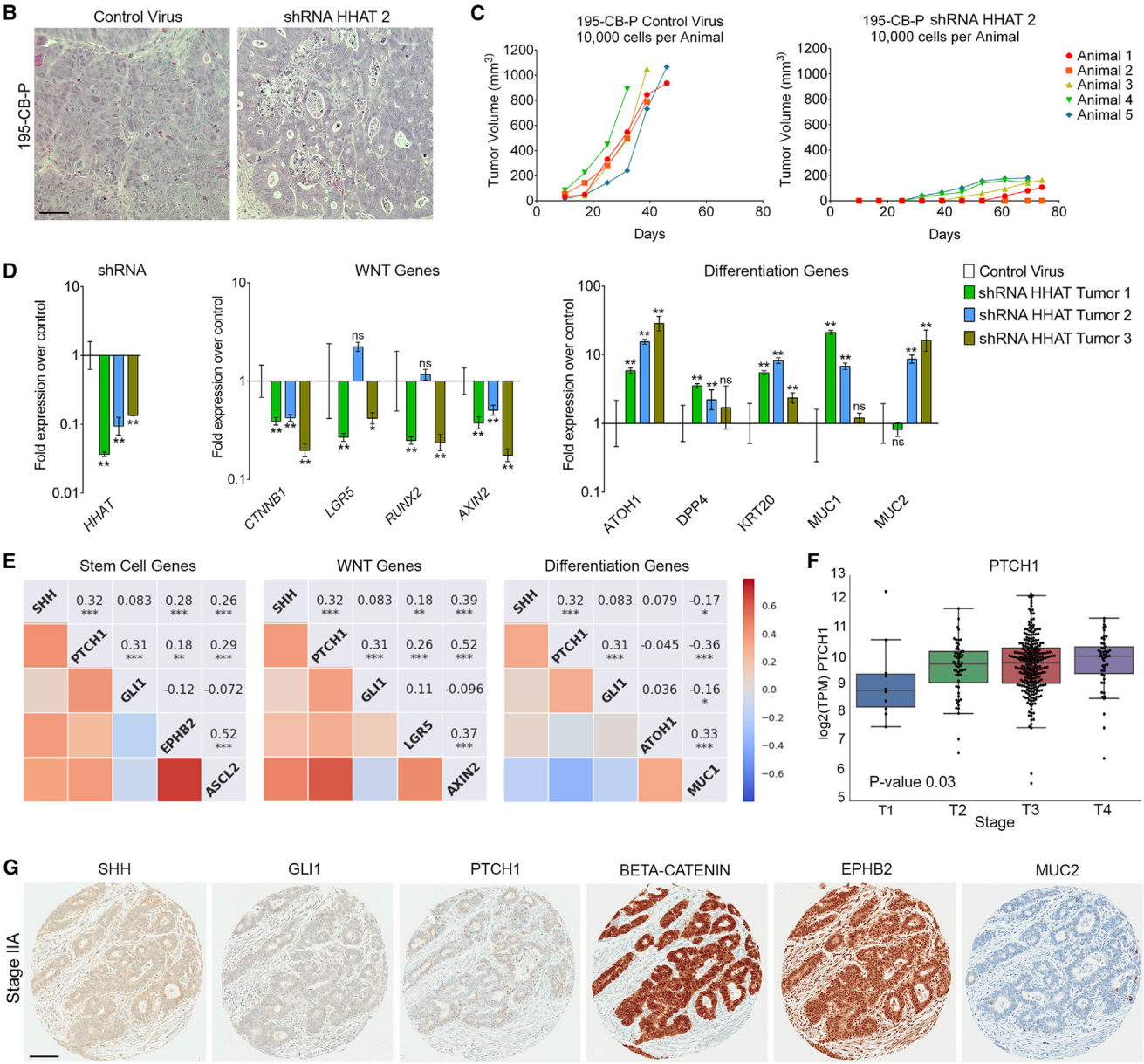

(legend on next page)

and nominal p values. $p < 0.05$ was considered statistically significant. Pairwise correlations were analyzed with Pearson correlation test.

DATA AND SOFTWARE AVAILABILITY

The accession number for the RNA sequencing data reported in this paper is ArrayExpress: E-MTAB-5209.

SUPPLEMENTAL INFORMATION

Supplemental Information includes Supplemental Experimental Procedures, seven figures, four tables, and two movies and can be found with this article online at https://doi.org/10.1016/j.celrep.2017.11.025.

AUTHOR CONTRIBUTIONS

Conceptualization, J.L.R. and M.L.; Methodology, J.L.R. and M.L.; Investigation, J.L.R., D.S., S.S., A.S., J.H., N.G.-S., C.S., and M.L.; Writing – Original Draft, J.L.R.; Writing – Review & Editing, J.L.R. and M.L.; Data Curation, A.S.; Resources, J.H., U.K., and C.R.A.R.; Supervision, D.M., D.H., H.L., R.S., and M.L.

ACKNOWLEDGMENTS

We thank Ralf Lesche and Joern Toedling (Bayer AG, Berlin, Germany) for support with RNA sequencing; Elissaveta Petrova (Merck, Germany) and Marie-Laure Yaspo (Max Planck Institute for Molecular Genetics, Berlin, Germany) for helpful discussions and comments on the manuscript; and Thibaud Jourdan (Bayer AG, Berlin, Germany), Dorothea Przybilla, and Cathrin Davies (Laboratory of Molecular Tumor Pathology, Charité Universitätsmedizin Berlin, Germany) for technical and cell culture assistance. The research leading to these results has received support from the Innovative Medicines Initiative Joint Undertaking under Grant Agreement 115234 (OncoTrack), the resources of which are composed of financial contribution from the European Union Seventh Framework Programme (FP7/2007-2013) and EFPIA companies in kind contribution. J.L.R., A.S., D.M., D.H., and M.L. are employees or shareholders of Bayer AG. H.L. is the founder of Alacris Theranostics. R.S. and C.R.A.R. are founders of cpo.

Received: July 12, 2017
Revised: August 15, 2017
Accepted: November 6, 2017
Published: December 5, 2017

REFERENCES

Akiyoshi, T., Nakamura, M., Koga, K., Nakashima, H., Yao, T., Tsuneyoshi, M., Tanaka, M., and Katano, M. (2006). Gli1, downregulated in colorectal cancers, inhibits proliferation of colon cancer cells involving Wnt signalling activation. Gut *55*, 991–999.

Aragaki, M., Tsuchiya, K., Okamoto, R., Yoshioka, S., Nakamura, T., Sakamoto, N., Kanai, T., and Watanabe, M. (2008). Proteasomal degradation of Atoh1 by aberrant Wnt signaling maintains the undifferentiated state of colon cancer. Biochem. Biophys. Res. Commun. *368*, 923–929.

Barnes, E.A., Kong, M., Ollendorff, V., and Donoghue, D.J. (2001). Patched1 interacts with cyclin B1 to regulate cell cycle progression. EMBO J. *20*, 2214–2223.

Berlin, J., Bendell, J.C., Hart, L.L., Firdaus, I., Gore, I., Hermann, R.C., Mulcahy, M.F., Zalupski, M.M., Mackey, H.M., Yauch, R.L., et al. (2013). A randomized phase II trial of vismodegib versus placebo with FOLFOX or FOLFIRI and bevacizumab in patients with previously untreated metastatic colorectal cancer. Clin. Cancer Res. *19*, 258–267.

Berman, D.M., Karhadkar, S.S., Maitra, A., Montes De Oca, R., Gerstenblith, M.R., Briggs, K., Parker, A.R., Shimada, Y., Eshleman, J.R., Watkins, D.N., and Beachy, P.A. (2003). Widespread requirement for Hedgehog ligand stimulation in growth of digestive tract tumours. Nature *425*, 846–851.

Bossuyt, W., Kazanjian, A., De Geest, N., Van Kelst, S., De Hertogh, G., Geboes, K., Boivin, G.P., Luciani, J., Fuks, F., Chuah, M., et al. (2009). Atonal homolog 1 is a tumor suppressor gene. PLoS Biol. *7*, e39.

Brennan, D., Chen, X., Cheng, L., Mahoney, M., and Riobo, N.A. (2012). Noncanonical Hedgehog signaling. Vitam. Horm. *88*, 55–72.

Briscoe, J., and Thérond, P.P. (2013). The mechanisms of Hedgehog signalling and its roles in development and disease. Nat. Rev. Mol. Cell Biol. *14*, 416–429.

Cancer Genome Atlas Network (2012). Comprehensive molecular characterization of human colon and rectal cancer. Nature *487*, 330–337.

Catenacci, D.V., Junttila, M.R., Karrison, T., Bahary, N., Horiba, M.N., Nattam, S.R., Marsh, R., Wallace, J., Kozloff, M., Rajdev, L., et al. (2015). Randomized Phase Ib/II Study of Gemcitabine Plus Placebo or Vismodegib, a Hedgehog Pathway Inhibitor, in Patients With Metastatic Pancreatic Cancer. J. Clin. Oncol. *33*, 4284–4292.

Chatel, G., Ganeff, C., Boussif, N., Delacroix, L., Briquet, A., Nolens, G., and Winkler, R. (2007). Hedgehog signaling pathway is inactive in colorectal cancer cell lines. Int. J. Cancer *121*, 2622–2627.

Chen, M.H., Li, Y.J., Kawakami, T., Xu, S.M., and Chuang, P.T. (2004). Palmitoylation is required for the production of a soluble multimeric Hedgehog protein complex and long-range signaling in vertebrates. Genes Dev. *18*, 641–659.

Chinchilla, P., Xiao, L., Kazanietz, M.G., and Riobo, N.A. (2010). Hedgehog proteins activate pro-angiogenic responses in endothelial cells through non-canonical signaling pathways. Cell Cycle *9*, 570–579.

Clevers, H. (2016). Modeling Development and Disease with Organoids. Cell *165*, 1586–1597.

Cumming, G., Fidler, F., and Vaux, D.L. (2007). Error bars in experimental biology. J. Cell Biol. *177*, 7–11.

Douville, J., Beaulieu, R., and Balicki, D. (2009). ALDH1 as a functional marker of cancer stem and progenitor cells. Stem Cells Dev. *18*, 17–25.

Dutta, D., Heo, I., and Clevers, H. (2017). Disease Modeling in Stem Cell-Derived 3D Organoid Systems. Trends Mol. Med *23*, 393–410.

Figure 7. Non-canonical Hedgehog Signaling Is Required for Tumorigenesis and Regulates the Differentiation of Colon CSCs *In Vivo*

(A) The table shows results of limiting dilution transplantation of control virus-transduced and shRNA HHAT-transduced 195-CB-P and 278-ML-P cells. The number of established tumors as a fraction of the number of animals transplanted is given. The p values for pairwise tests of differences in TIC frequencies between control virus versus shRNA HHAT 1, shRNA HHAT 2, and shRNA HHAT 3 278-ML-P cells are 3.78×10^{-8}, 4.53×10^{-8}, and 6.9×10^{-9}, respectively, and in 195-CB-P cells are 3.72×10^{-10}, 1.22×10^{-4}, and 1.23×10^{-5}, respectively.

(B) H&E staining of control and shRNA HHAT tissue (scale bar, 100 μm).

(C) Growth curves for xenografts derived from control virus-transduced cells and shRNA HHAT-transduced cells.

(D) Fold expression of *HHAT*, WNT, and differentiation RT-PCR gene expression data ± 95% CIs in four separate 195-CB-P shRNA HHAT tumors over the comparator population (four control virus-transduced 195-CB-P xenografts) (see also Table S4). Significant differences are as follows: *$p < 0.05$, **$p < 0.01$.

(E) Pairwise correlation of Hedgehog genes (*SHH*, *PTCH1*, and *GLI1*) with stem cell genes (*EPHB2* and *ASCL2*), WNT genes (*LGR5* and *AXIN2*), and differentiation genes (*ATOH1* and *MUC1*) in clinical samples.

(F) Expression of *PTCH1* in colorectal cancer patients across different tumor stages (T1 v T4, $p = 0.03$).

(G) Immunostaining of a stage IIA primary patient colorectal tumor for SHH, GLI1, PTCH1, BETA-CATENIN, EPHB2, and MUC2 (scale bar, 200 μm) (see also Figure S7).

Goodrich, L.V., Johnson, R.L., Milenkovic, L., McMahon, J.A., and Scott, M.P. (1996). Conservation of the hedgehog/patched signaling pathway from flies to mice: induction of a mouse patched gene by Hedgehog. Genes Dev. *10*, 301–312.

Haggar, F.A., and Boushey, R.P. (2009). Colorectal cancer epidemiology: incidence, mortality, survival, and risk factors. Clin. Colon Rectal Surg. *22*, 191–197.

Hebenstreit, D., Fang, M., Gu, M., Charoensawan, V., van Oudenaarden, A., and Teichmann, S.A. (2011). RNA sequencing reveals two major classes of gene expression levels in metazoan cells. Mol. Syst. Biol. *7*, 497.

Hu, Y., and Smyth, G.K. (2009). ELDA: extreme limiting dilution analysis for comparing depleted and enriched populations in stem cell and other assays. J. Immunol. Methods *347*, 70–78.

Huang, E.H., Hynes, M.J., Zhang, T., Ginestier, C., Dontu, G., Appelman, H., Fields, J.Z., Wicha, M.S., and Boman, B.M. (2009). Aldehyde dehydrogenase 1 is a marker for normal and malignant human colonic stem cells (SC) and tracks SC overpopulation during colon tumorigenesis. Cancer Res. *69*, 3382–3389.

Ingham, P.W. (1998). The patched gene in development and cancer. Curr. Opin. Genet. Dev. *8*, 88–94.

Kanwar, S.S., Yu, Y., Nautiyal, J., Patel, B.B., and Majumdar, A.P. (2010). The Wnt/beta-catenin pathway regulates growth and maintenance of colonospheres. Mol. Cancer *9*, 212.

Karamboulas, C., and Ailles, L. (2013). Developmental signaling pathways in cancer stem cells of solid tumors. Biochim. Biophys. Acta *1830*, 2481–2495.

Kolterud, A., Grosse, A.S., Zacharias, W.J., Walton, K.D., Kretovich, K.E., Madison, B.B., Waghray, M., Ferris, J.E., Hu, C., Merchant, J.L., et al. (2009). Paracrine Hedgehog signaling in stomach and intestine: new roles for hedgehog in gastrointestinal patterning. Gastroenterology *137*, 618–628.

Krausova, M., and Korinek, V. (2014). Wnt signaling in adult intestinal stem cells and cancer. Cell. Signal. *26*, 570–579.

Kreso, A., van Galen, P., Pedley, N.M., Lima-Fernandes, E., Frelin, C., Davis, T., Cao, L., Baiazitov, R., Du, W., Sydorenko, N., et al. (2014). Self-renewal as a therapeutic target in human colorectal cancer. Nat. Med. *20*, 29–36.

Madison, B.B., Braunstein, K., Kuizon, E., Portman, K., Qiao, X.T., and Gumucio, D.L. (2005). Epithelial hedgehog signals pattern the intestinal crypt-villus axis. Development *132*, 279–289.

Marigo, V., and Tabin, C.J. (1996). Regulation of patched by sonic hedgehog in the developing neural tube. Proc. Natl. Acad. Sci. USA *93*, 9346–9351.

Matevossian, A., and Resh, M.D. (2015). Hedgehog Acyltransferase as a target in estrogen receptor positive, HER2 amplified, and tamoxifen resistant breast cancer cells. Mol. Cancer *14*, 72.

Mehlen, P., and Bredesen, D.E. (2004). The dependence receptor hypothesis. Apoptosis *9*, 37–49.

Merlos-Suárez, A., Barriga, F.M., Jung, P., Iglesias, M., Céspedes, M.V., Rossell, D., Sevillano, M., Hernando-Momblona, X., da Silva-Diz, V., Muñoz, P., et al. (2011). The intestinal stem cell signature identifies colorectal cancer stem cells and predicts disease relapse. Cell Stem Cell *8*, 511–524.

Mille, F., Thibert, C., Fombonne, J., Rama, N., Guix, C., Hayashi, H., Corset, V., Reed, J.C., and Mehlen, P. (2009). The Patched dependence receptor triggers apoptosis through a DRAL-caspase-9 complex. Nat. Cell Biol. *11*, 739–746.

Miyaki, M., Konishi, M., Kikuchi-Yanoshita, R., Enomoto, M., Igari, T., Tanaka, K., Muraoka, M., Takahashi, H., Amada, Y., Fukayama, M., et al. (1994). Characteristics of somatic mutation of the adenomatous polyposis coli gene in colorectal tumors. Cancer Res. *54*, 3011–3020.

Mootha, V.K., Lindgren, C.M., Eriksson, K.F., Subramanian, A., Sihag, S., Lehar, J., Puigserver, P., Carlsson, E., Ridderstråle, M., Laurila, E., et al. (2003). PGC-1alpha-responsive genes involved in oxidative phosphorylation are coordinately downregulated in human diabetes. Nat. Genet. *34*, 267–273.

Nolan-Stevaux, O., Lau, J., Truitt, M.L., Chu, G.C., Hebrok, M., Fernández-Zapico, M.E., and Hanahan, D. (2009). GLI1 is regulated through Smoothened-independent mechanisms in neoplastic pancreatic ducts and mediates PDAC cell survival and transformation. Genes Dev. *23*, 24–36.

Nusse, R. (2008). Wnt signaling and stem cell control. Cell Res. *18*, 523–527.

O'Brien, C.A., Pollett, A., Gallinger, S., and Dick, J.E. (2007). A human colon cancer cell capable of initiating tumour growth in immunodeficient mice. Nature *445*, 106–110.

Oniscu, A., James, R.M., Morris, R.G., Bader, S., Malcomson, R.D., and Harrison, D.J. (2004). Expression of Sonic hedgehog pathway genes is altered in colonic neoplasia. J. Pathol. *203*, 909–917.

Park, J., Zhang, J.J., Moro, A., Kushida, M., Wegner, M., and Kim, P.C. (2010). Regulation of Sox9 by Sonic Hedgehog (Shh) is essential for patterning and formation of tracheal cartilage. Dev. Dyn. *239*, 514–526.

Petrova, E., Matevossian, A., and Resh, M.D. (2015). Hedgehog acyltransferase as a target in pancreatic ductal adenocarcinoma. Oncogene *34*, 263–268.

Pinto, D., Gregorieff, A., Begthel, H., and Clevers, H. (2003). Canonical Wnt signals are essential for homeostasis of the intestinal epithelium. Genes Dev. *17*, 1709–1713.

Polizio, A.H., Chinchilla, P., Chen, X., Manning, D.R., and Riobo, N.A. (2011). Sonic Hedgehog activates the GTPases Rac1 and RhoA in a Gli-independent manner through coupling of smoothened to Gi proteins. Sci. Signal. *4*, pt7.

Reya, T., Morrison, S.J., Clarke, M.F., and Weissman, I.L. (2001). Stem cells, cancer, and cancer stem cells. Nature *414*, 105–111.

Ricci-Vitiani, L., Lombardi, D.G., Pilozzi, E., Biffoni, M., Todaro, M., Peschle, C., and De Maria, R. (2007). Identification and expansion of human colon-cancer-initiating cells. Nature *445*, 111–115.

Roberts, D.J., Johnson, R.L., Burke, A.C., Nelson, C.E., Morgan, B.A., and Tabin, C. (1995). Sonic hedgehog is an endodermal signal inducing Bmp-4 and Hox genes during induction and regionalization of the chick hindgut. Development *121*, 3163–3174.

Sakthianandeswaren, A., Christie, M., D'Andreti, C., Tsui, C., Jorissen, R.N., Li, S., Fleming, N.I., Gibbs, P., Lipton, L., Malaterre, J., et al. (2011). PHLDA1 expression marks the putative epithelial stem cells and contributes to intestinal tumorigenesis. Cancer Res. *71*, 3709–3719.

Sato, T., Stange, D.E., Ferrante, M., Vries, R.G., Van Es, J.H., Van den Brink, S., Van Houdt, W.J., Pronk, A., Van Gorp, J., Siersema, P.D., and Clevers, H. (2011). Long-term expansion of epithelial organoids from human colon, adenoma, adenocarcinoma, and Barrett's epithelium. Gastroenterology *141*, 1762–1772.

Scales, S.J., and de Sauvage, F.J. (2009). Mechanisms of Hedgehog pathway activation in cancer and implications for therapy. Trends Pharmacol. Sci. *30*, 303–312.

Schuijers, J., Junker, J.P., Mokry, M., Hatzis, P., Koo, B.K., Sasselli, V., van der Flier, L.G., Cuppen, E., van Oudenaarden, A., and Clevers, H. (2015). Ascl2 acts as an R-spondin/Wnt-responsive switch to control stemness in intestinal crypts. Cell Stem Cell *16*, 158–170.

Schütte, M., Risch, T., Abdavi-Azar, N., Boehnke, K., Schumacher, D., Keil, M., Yildiriman, R., Jandrasits, C., Borodina, T., Amstislavskiy, V., et al. (2017). Molecular dissection of colorectal cancer in pre-clinical models identifies biomarkers predicting sensitivity to EGFR inhibitors. Nat. Commun. *8*, 14262.

Shackleton, M., Quintana, E., Fearon, E.R., and Morrison, S.J. (2009). Heterogeneity in cancer: cancer stem cells versus clonal evolution. Cell *138*, 822–829.

Shenoy, A., Butterworth, E., and Huang, E.H. (2012). ALDH as a marker for enriching tumorigenic human colonic stem cells. Methods Mol. Biol. *916*, 373–385.

Shroyer, N.F., Helmrath, M.A., Wang, V.Y., Antalffy, B., Henning, S.J., and Zoghbi, H.Y. (2007). Intestine-specific ablation of mouse atonal homolog 1 (Math1) reveals a role in cellular homeostasis. Gastroenterology *132*, 2478–2488.

Siegel, R., Desantis, C., and Jemal, A. (2014). Colorectal cancer statistics, 2014. CA Cancer J. Clin. *64*, 104–117.

Song, L., Li, Z.Y., Liu, W.P., and Zhao, M.R. (2015). Crosstalk between Wnt/β-catenin and Hedgehog/Gli signaling pathways in colon cancer and implications for therapy. Cancer Biol. Ther. *16*, 1–7.

Subramanian, A., Tamayo, P., Mootha, V.K., Mukherjee, S., Ebert, B.L., Gillette, M.A., Paulovich, A., Pomeroy, S.L., Golub, T.R., Lander, E.S., and Mesirov, J.P. (2005). Gene set enrichment analysis: a knowledge-based approach for interpreting genome-wide expression profiles. Proc. Natl. Acad. Sci. USA *102*, 15545–15550.

Taipale, J., and Beachy, P.A. (2001). The Hedgehog and Wnt signalling pathways in cancer. Nature *411*, 349–354.

Testaz, S., Jarov, A., Williams, K.P., Ling, L.E., Koteliansky, V.E., Fournier-Thibault, C., and Duband, J.L. (2001). Sonic hedgehog restricts adhesion and migration of neural crest cells independently of the Patched- Smoothened-Gli signaling pathway. Proc. Natl. Acad. Sci. USA *98*, 12521–12526.

Thibert, C., Teillet, M.A., Lapointe, F., Mazelin, L., Le Douarin, N.M., and Mehlen, P. (2003). Inhibition of neuroepithelial patched-induced apoptosis by sonic hedgehog. Science *301*, 843–846.

van de Wetering, M., Francies, H.E., Francis, J.M., Bounova, G., Iorio, F., Pronk, A., van Houdt, W., van Gorp, J., Taylor-Weiner, A., Kester, L., et al. (2015). Prospective derivation of a living organoid biobank of colorectal cancer patients. Cell *161*, 933–945.

van den Brink, G.R., and Hardwick, J.C. (2006). Hedgehog Wnteraction in colorectal cancer. Gut *55*, 912–914.

van den Brink, G.R., Bleuming, S.A., Hardwick, J.C., Schepman, B.L., Offerhaus, G.J., Keller, J.J., Nielsen, C., Gaffield, W., van Deventer, S.J., Roberts, D.J., and Peppelenbosch, M.P. (2004). Indian Hedgehog is an antagonist of Wnt signaling in colonic epithelial cell differentiation. Nat. Genet. *36*, 277–282.

van der Flier, L.G., Haegebarth, A., Stange, D.E., van de Wetering, M., and Clevers, H. (2009). OLFM4 is a robust marker for stem cells in human intestine and marks a subset of colorectal cancer cells. Gastroenterology *137*, 15–17.

Van Dop, W.A., Uhmann, A., Wijgerde, M., Sleddens-Linkels, E., Heijmans, J., Offerhaus, G.J., van den Bergh Weerman, M.A., Boeckxstaens, G.E., Hommes, D.W., Hardwick, J.C., et al. (2009). Depletion of the colonic epithelial precursor cell compartment upon conditional activation of the hedgehog pathway. Gastroenterology *136*, 2195–2203, e1–7.

Varnat, F., Duquet, A., Malerba, M., Zbinden, M., Mas, C., Gervaz, P., and Ruiz i Altaba, A. (2009). Human colon cancer epithelial cells harbour active HEDGEHOG-GLI signalling that is essential for tumour growth, recurrence, metastasis and stem cell survival and expansion. EMBO Mol. Med. *1*, 338–351.

Vermeulen, L., Sprick, M.R., Kemper, K., Stassi, G., and Medema, J.P. (2008). Cancer stem cells–old concepts, new insights. Cell Death Differ. *15*, 947–958.

Vermeulen, L., De Sousa E Melo, F., van der Heijden, M., Cameron, K., de Jong, J.H., Borovski, T., Tuynman, J.B., Todaro, M., Merz, C., Rodermond, H., et al. (2010). Wnt activity defines colon cancer stem cells and is regulated by the microenvironment. Nat. Cell Biol. *12*, 468–476.

Vogel, C., and Marcotte, E.M. (2012). Insights into the regulation of protein abundance from proteomic and transcriptomic analyses. Nat. Rev. Genet. *13*, 227–232.

Wang, X., Venugopal, C., Manoranjan, B., McFarlane, N., O'Farrell, E., Nolte, S., Gunnarsson, T., Hollenberg, R., Kwiecien, J., Northcott, P., et al. (2012). Sonic hedgehog regulates Bmi1 in human medulloblastoma brain tumor-initiating cells. Oncogene *31*, 187–199.

Weiswald, L.B., Bellet, D., and Dangles-Marie, V. (2015). Spherical cancer models in tumor biology. Neoplasia *17*, 1–15.

Wong, V.W., Stange, D.E., Page, M.E., Buczacki, S., Wabik, A., Itami, S., van de Wetering, M., Poulsom, R., Wright, N.A., Trotter, M.W., et al. (2012). Lrig1 controls intestinal stem-cell homeostasis by negative regulation of ErbB signalling. Nat. Cell Biol. *14*, 401–408.

Wu, Z.Q., Brabletz, T., Fearon, E., Willis, A.L., Hu, C.Y., Li, X.Y., and Weiss, S.J. (2012). Canonical Wnt suppressor, Axin2, promotes colon carcinoma oncogenic activity. Proc. Natl. Acad. Sci. USA *109*, 11312–11317.

Xu, X., Su, B., Xie, C., Wei, S., Zhou, Y., Liu, H., Dai, W., Cheng, P., Wang, F., Xu, X., and Guo, C. (2014). Sonic hedgehog-Gli1 signaling pathway regulates the epithelial mesenchymal transition (EMT) by mediating a new target gene, S100A4, in pancreatic cancer cells. PLoS ONE *9*, e96441.

Yang, Q., Bermingham, N.A., Finegold, M.J., and Zoghbi, H.Y. (2001). Requirement of Math1 for secretory cell lineage commitment in the mouse intestine. Science *294*, 2155–2158.

Yauch, R.L., Gould, S.E., Scales, S.J., Tang, T., Tian, H., Ahn, C.P., Marshall, D., Fu, L., Januario, T., Kallop, D., et al. (2008). A paracrine requirement for hedgehog signalling in cancer. Nature *455*, 406–410.

Yoshikawa, K., Shimada, M., Miyamoto, H., Higashijima, J., Miyatani, T., Nishioka, M., Kurita, N., Iwata, T., and Uehara, H. (2009). Sonic hedgehog relates to colorectal carcinogenesis. J. Gastroenterol. *44*, 1113–1117.

Yoshimoto, A.N., Bernardazzi, C., Carneiro, A.J., Elia, C.C., Martinusso, C.A., Ventura, G.M., Castelo-Branco, M.T., and de Souza, H.S. (2012). Hedgehog pathway signaling regulates human colon carcinoma HT-29 epithelial cell line apoptosis and cytokine secretion. PLoS ONE *7*, e45332.

Yoshino, T., Murai, H., and Saito, D. (2016). Hedgehog-BMP signalling establishes dorsoventral patterning in lateral plate mesoderm to trigger gonadogenesis in chicken embryos. Nat. Commun. *7*, 12561.

You, S., Zhou, J., Chen, S., Zhou, P., Lv, J., Han, X., and Sun, Y. (2010). PTCH1, a receptor of Hedgehog signaling pathway, is correlated with metastatic potential of colorectal cancer. Ups. J. Med. Sci. *115*, 169–175.

Cell Reports, Volume *21*

Supplemental Information

Non-Canonical Hedgehog Signaling Is a Positive Regulator of the WNT Pathway and Is Required for the Survival of Colon Cancer Stem Cells

Joseph L. Regan, Dirk Schumacher, Stephanie Staudte, Andreas Steffen, Johannes Haybaeck, Ulrich Keilholz, Caroline Schweiger, Nicole Golob-Schwarzl, Dominik Mumberg, David Henderson, Hans Lehrach, Christian R.A. Regenbrecht, Reinhold Schäfer, and Martin Lange

Supplemental Information

Supplemental Experimental Procedures

Supplemental Figures and Tables

Supplemental References

Supplemental Experimental Procedures

Histology and immunohistochemistry

Tumors were fixed in 4% paraformaldehyde overnight for routine histological analysis and immunohistochemistry. Immunohistochemistry was carried out via standard techniques with MKI67 (HPA001164, rabbit polyclonal, Sigma; diluted 1:250), SHH (NBP1-69270, rabbit polyclonal, Novusbio, diluted 1:50), SMO (ab38686, rabbit polyclonal, Abcam, diluted 1:120), BMI1 (#6964, rabbit monoclonal, Cell Signaling Technology; diluted 1:400), GLI1 (ab49314, rabbit polyclonal, Abcam, diluted 1:250), Non-phospho (Active) β-Catenin (#8814, rabbit monoclonal, Cell Signaling, diluted 1:800), EPHB2 (PA5-14607, rabbit polyclonal, Thermo Fisher, 1:200), PTCH1 (NBP1-47945, mouse monoclonal, Novus, 1:200), BMI1 (#6964, rabbit monoclonal, Cell Signaling Technology; diluted 1:200), and MUC2 (#2900-1, rabbit monoclonal, Epitomics, 1:500) antibodies. Negative controls were performed using the same protocols with substitution of the primary antibody with IgG-matched controls (ab172730, rabbit IgG, monoclonal [EPR25A], Abcam and ab91353, mouse IgG1 monoclonal [ICIGG1], Abcam isotype controls). Tissue microarrays containing samples from 75 colorectal cancer patients from the OncoTrack cohort [1] were obtained from The Institute of Pathology, Medical University Graz (Auenbruggerplatz 25, 8036, Graz, Austria) and analyzed using Aperio TMALab and Image software (Leica Biosystems).

Immunofluorescence staining of cancer organoids

For immunofluorescence imaging, cancer organoid cultures were fixed in 4% paraformaldehyde for 30 min at room temperature and permeabilized with 0.1% Triton X-100 for 30 min. Samples were blocked in phosphate-buffered saline (PBS) with 10% bovine serum albumin (BSA). Samples were incubated with primary antibodies overnight at 4^{o}C. Antibodies used were Non-phospho (Active) β-Catenin (Ser33/37/Thr41) (D13A1) (#8814, rabbit monoclonal, Cell Signaling Technology; diluted 1:200), KRT20 (HPA024684, rabbit polyclonal, Sigma; diluted 1:200), SHH (NBP1-69270, rabbit polyclonal, Novus Biologicals; diluted 1:200), SMO (ab38686, rabbit polyclonal, Abcam; diluted 1:200), BMI1 (D20B7) XP® (#6964, rabbit monoclonal, Cell Signaling Technology; diluted 1:200), GLI1 (ab49314, rabbit polyclonal, Abcam; diluted 1:200) and PTCH1 (5c7) (NBP1-47945, mouse monoclonal, Novus Biologicals; 1:100). Samples were stained with a conjugated secondary antibody overnight at 4 ^{o}C. F-actin was stained with Alexa Fluor® 647 Phalloidin (#A22287, Thermo Fisher; diluted 1:20) for 30 min at room temperature. Nuclei were counterstained with DAPI. Negative controls were performed using the same protocol with substitution of the primary antibody with IgG-matched controls. Cancer organoids were then transferred to microscope slides for examination using a Zeiss LSM 700 Laser Scanning Microscope.

Limiting dilution spheroid assays

Cancer organoids were dissociated to single cells and sorted by FACS, using DAPI to exclude dead cells, into 96-well ultra-low attachment plates. 20 days later, wells containing spheroids were counted and used to calculate the CSC frequency using the ELDA software. ImageJ software was used to calculate sphere size. For shRNA HHAT spheroid assays, transduced cancer organoids were dissociated and live ($DAPI^{Negative}$ $GFP^{Positive}$) cells were sorted at 100 cells per well into 96-well ultra-low attachment plates. For siRNA spheroid assays, live ($DAPI^{Negative}$) cells were sorted at 10 cells per well into 96-well ultra-low attachment plates.

Aldefluor Assay

Organoids and xenografts were processed to single cells and labelled using the Aldefluor Assay according to manufacturer's (Stemcell Technologies) instructions. GFP expressing cells were labelled using the AldeRed (a red-shifted fluorescent substrate for ALDH used for labelling viable ALDH positive cells that does not interfere with the GFP emission channel) ALDH Detection Assay (SCR150, Merck Millipore). ALDH levels were assessed by FACS on a BD LSR II analyzer.

RNA Sequencing

Cells were lysed in RLT buffer and processed for RNA using the RNeasy Mini Plus RNA extraction kit (Qiagen). Samples were processed using Illumina's TrueSeq RNA protocol and sequenced on an Illumina HiSeq 2500 machine as 2x125nt paired-end reads. The raw data in Fastq format were checked for sample quality using our internal NGS

QC pipeline. Reads were mapped to the human reference genome (assembly hg19) using the STAR aligner (version 2.4.2a). Total read counts per gene were computed using the program "featureCounts" (version 1.4.6-p2) in the "subread" package, with the gene annotation taken from Gencode (version 19). The "DESeq2" Bioconductor package was used for the differential-expression analysis.

Small molecule inhibitor studies

Cancer organoids were dissociated to single cells and seeded in 10 µl Matrigel at 5 x 10^3 cells per well in 96-well plates and pre-cultured for 2 days to allow organoid formation prior to compound treatment. Cancer organoids were then treated with tankyrase (NVP-TNKS656), vismodegib, cyclopamine, RU-SKI 43 and 2 µg/ml recombinant human SHH (R&D Systems). Cell viability was determined using the CellTiter-Glo (Promega) cell viability assay after 72 h compound treatment.

Viral transduction

Cells were seeded in 100 µl volumes of antibiotic free culture media at 1 x 10^5 cells per well in ultra-low attachment 96-well plates. Control and shRNA lentiviruses were purchased from Sigma-Aldrich (Table S3). Viral particles were added at a multiplicity of infection of 1. Cells were transduced for up to 96 h or until GFP positive cells were observed before being embedded in Matrigel for the establishment of lentiviral transduced cancer organoid cultures. Puromycin (2 µg/ml) was used keep the cells under selection.

TCF/LEF-eGFP reporter assay

Lenti TCF/LEF reporter (Qiagen) is a preparation of replication incompetent, VSV-g pseudotyped lentivirus particles expressing the GFP gene under the control of a minimal (m)CMV promoter and tandem repeats of the TCF/LEF transcriptional response element (TRE). For the reporter assay, TCF/LEF-eGFP cancer organoids were pre-treated with 10 µM vismodegib or 2 µM RU-SKI 43 for 24 h. Control cells were incubated with equivalent concentrations of DMSO. Cancer organoids were then processed to single cells, stained for DAPI to exclude dead cells and analyzed by flow cytometry using the BD LSR II.

siRNA transfection

Single cells were seeded in 100 µl volumes of Accell™ Delivery Media (Dharmacon™) at 1 x 10^5 cells per well in ultra-low attachment 96-well plates and transfected with 2 µM concentrations of Accell™ siRNA SMO (E-005726-00-0005), siRNA PTCH1 (E-003924-00-0005) and control siRNA (Accell™ non-targeting siRNA control) (Dharmacon™) by incubating for up to 72 h.

Gene expression analysis

For quantitative real-time RT-PCR analysis RNA was isolated using the RNeasy Mini Plus RNA extraction kit (Qiagen). cDNA synthesis was carried out using a Sensiscript RT kit (Qiagen). RNA was transcribed into cDNA using an oligo dTn primer (Promega) per reaction. Gene expression analysis was performed using TaqMan® Gene Expression Assays (Applied Biosystems) (Table S4) on an ABI Prism 7900HT sequence detection system (Applied Biosystems). GAPDH was used as an endogenous control and results were calculated using the Δ-ΔCt method. Data were expressed as the mean fold gene expression difference in three independently isolated cell preparations over a comparator sample with 95% confidence intervals. Pairwise correlation studies were performed using the colorectal adenocarcinoma gene expression TCGA-COADREAD dataset (www.cBioPortal.org) including 382 patients with RNA-sequencing and clinical data.

Supplemental Figures and Tables

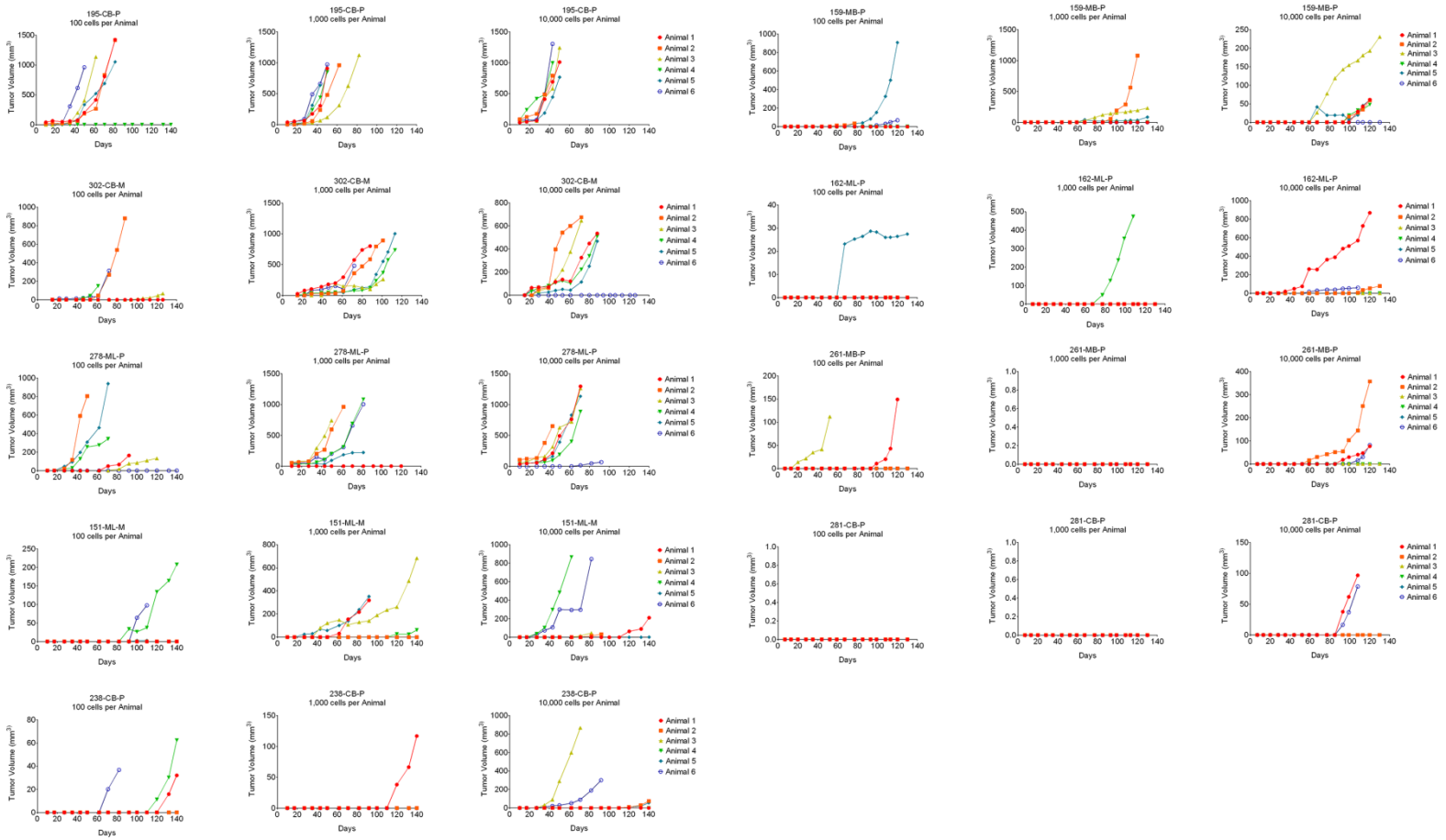

Figure S1 Limiting dilution tumor growth curves. Related to Figure 1.

Growth curves for nine xenograft models derived from 100, 1,000 and 10,000 cell dilution transplants.

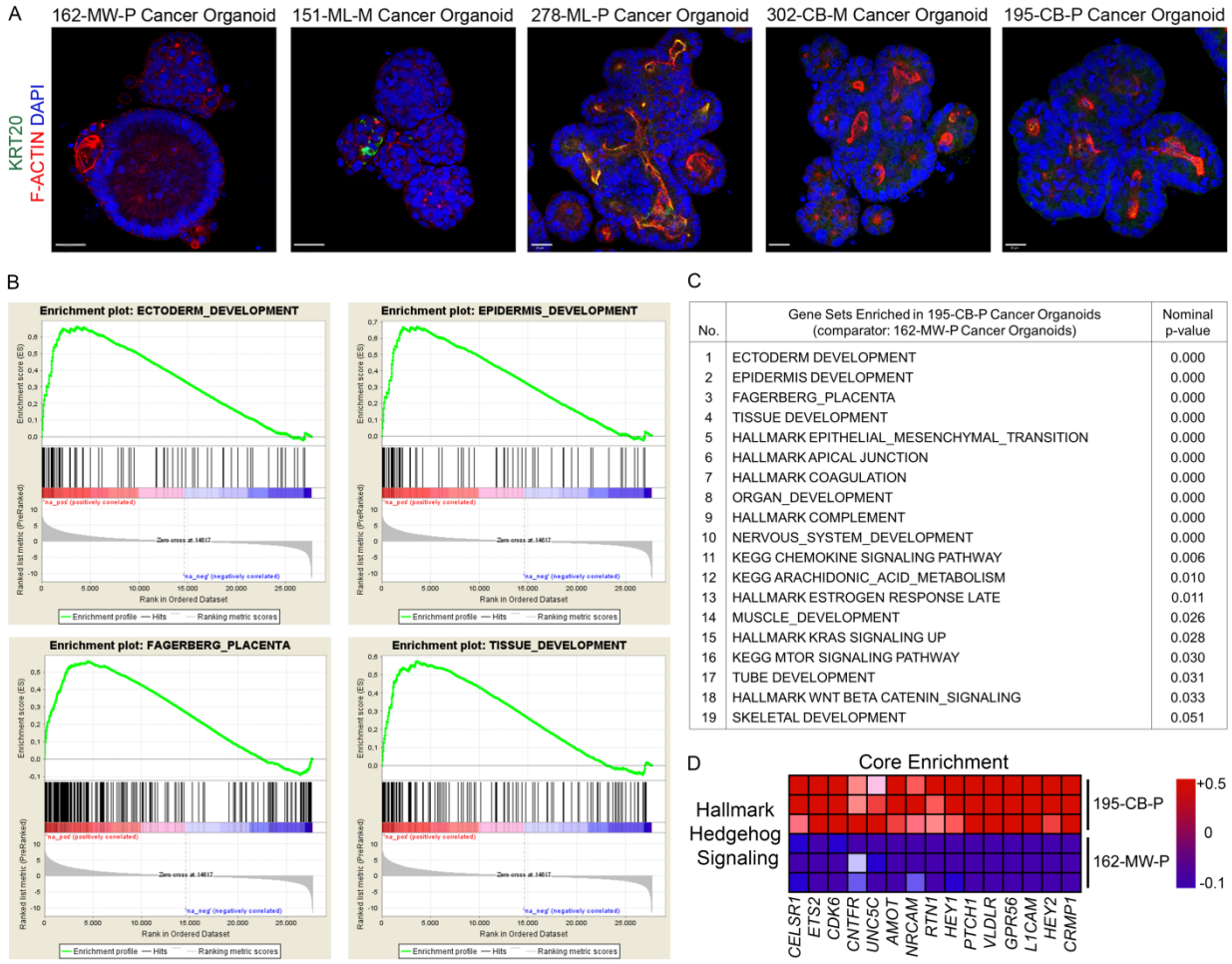

No.	Gene Sets Enriched in 195-CB-P Cancer Organoids (comparator: 162-MW-P Cancer Organoids)	Nominal p-value
1	ECTODERM DEVELOPMENT	0.000
2	EPIDERMIS DEVELOPMENT	0.000
3	FAGERBERG_PLACENTA	0.000
4	TISSUE DEVELOPMENT	0.000
5	HALLMARK EPITHELIAL_MESENCHYMAL_TRANSITION	0.000
6	HALLMARK APICAL JUNCTION	0.000
7	HALLMARK COAGULATION	0.000
8	ORGAN_DEVELOPMENT	0.000
9	HALLMARK COMPLEMENT	0.000
10	NERVOUS_SYSTEM_DEVELOPMENT	0.000
11	KEGG CHEMOKINE SIGNALING PATHWAY	0.006
12	KEGG ARACHIDONIC_ACID_METABOLISM	0.010
13	HALLMARK ESTROGEN RESPONSE LATE	0.011
14	MUSCLE_DEVELOPMENT	0.026
15	HALLMARK KRAS SIGNALING UP	0.028
16	KEGG MTOR SIGNALING PATHWAY	0.030
17	TUBE DEVELOPMENT	0.031
18	HALLMARK WNT BETA CATENIN_SIGNALING	0.033
19	SKELETAL DEVELOPMENT	0.051

Figure S2 CSC-enriched organoids have transcriptomes enriched for developmental gene sets. Related to Figure 2.

(A) Immunofluorescence staining of cancer organoids for pan-differentiation marker KRT20 (green) and F-ACTIN (red). Nuclei are stained blue with DAPI (Bars = 20 µm) (B) GSEA plots for ectoderm, epidermis, placental and tissue development and (C) list of gene sets enriched in CSC-enhanced 195-CB-P cancer organoids compared to CSC-depleted 162-MW-P cancer organoids. (D) Heat map showing core enrichment Hallmark Hedgehog signaling genes in 195-CB-P cells compared to 162-MW-P cells.

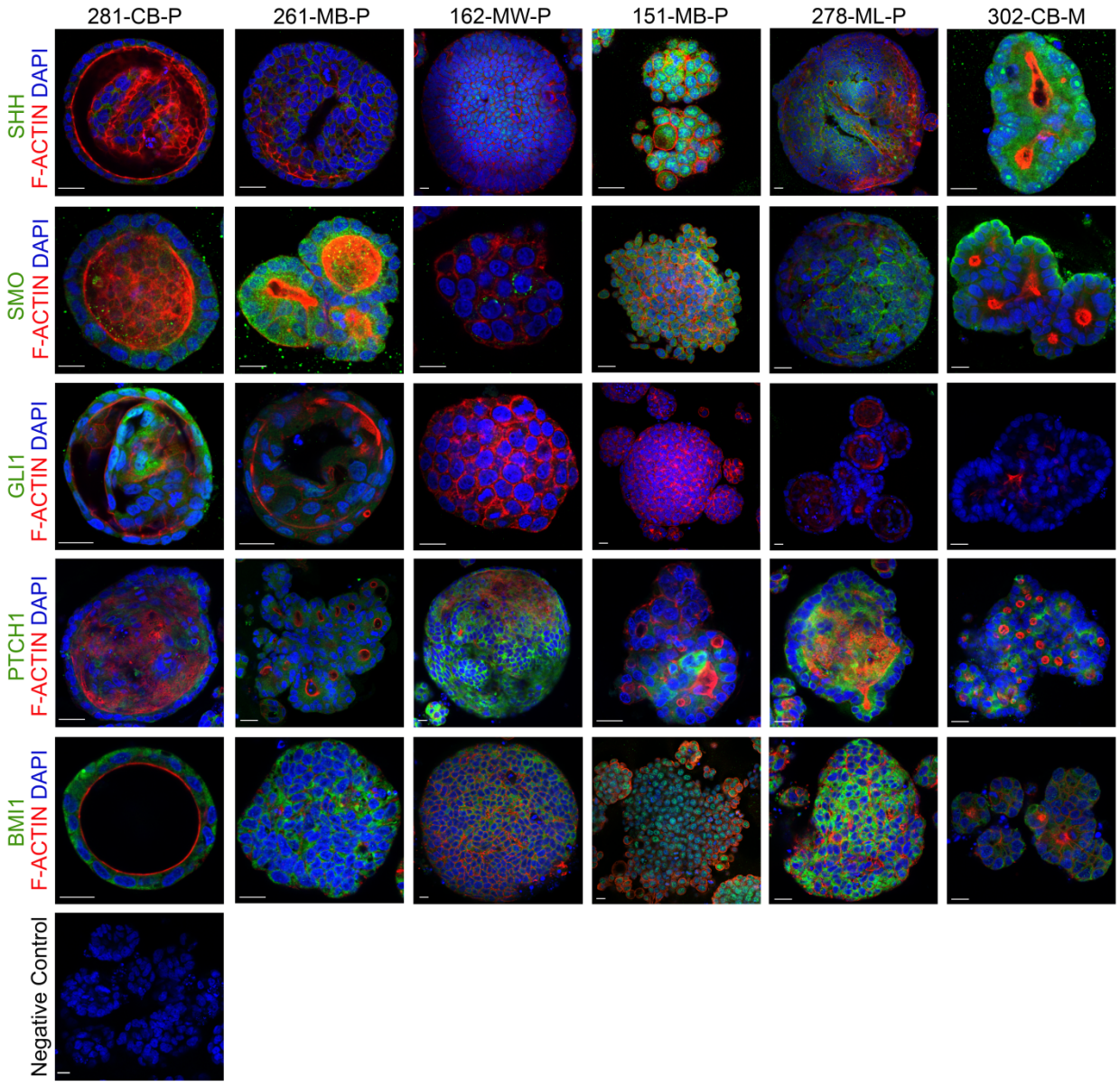

Figure S3 Hedgehog signaling in CSC-enriched colon cancer organoids is autocrine and GLI-independent. Related to Figure 3.

Immunostaining of cancer organoids for Hedgehog signaling proteins SHH, SMO, GLI1, PTCH1 and BMI1 (green) and F-ACTIN (red). Nuclei are stained blue with DAPI (Bars = 20 µm).

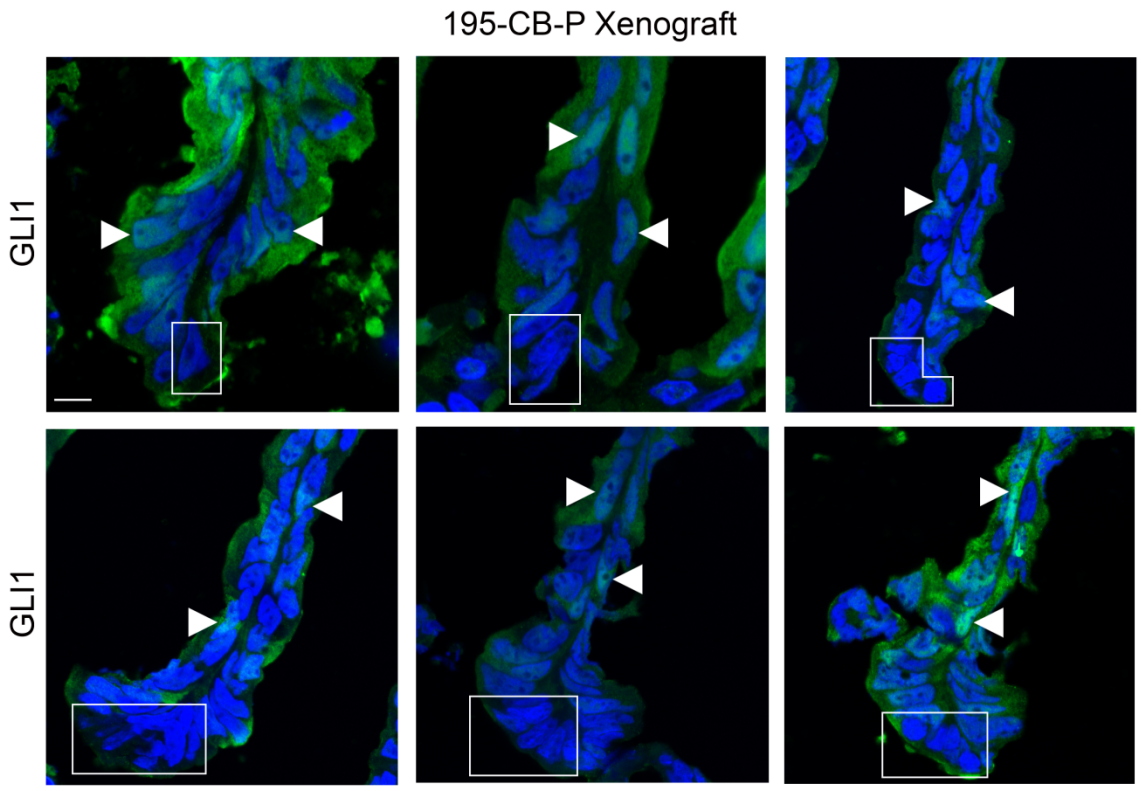

Figure S4 Nuclear GLI1 is not expressed at the base of "crypt-like" structures found in patient derived colon cancer xenografts. Related to Figure 3.

Immunofluorescence staining for GLI1 (green) in "crypt-like" structures in frozen 195-CB-P xenograft sections. Nuclei are stained blue with DAPI. Arrowheads indicate nuclear GLI1 staining. Boxes contain cells lacking nuclear GLI1 staining (Bars = 20 μm).

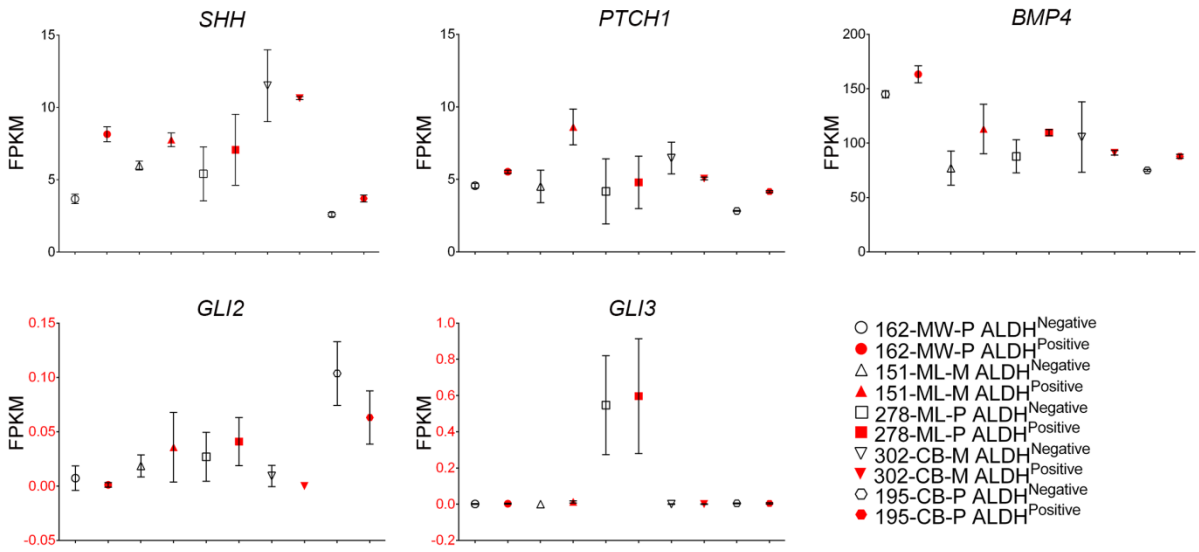

Figure S5 RNA sequencing generated FPKM values for *SHH*, *PTCH1*, *BMP4, GLI2* and *GLI3* in ALDH^{Positive} and ALDH^{Negative} cancer organoid cells. Related to Figure 4.

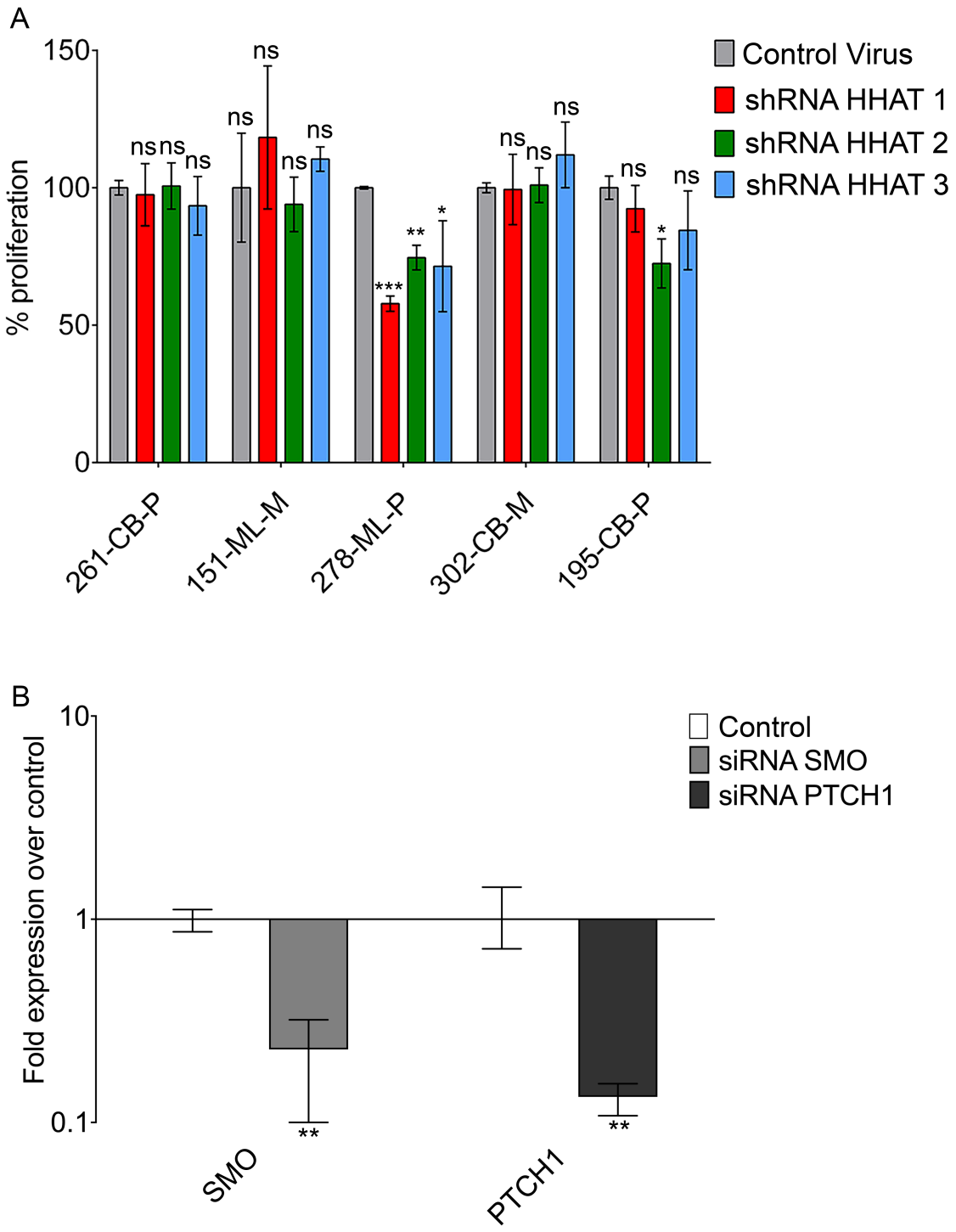

Figure S6 Viability of shRNA HHAT cancer organoids and demonstration of siRNA knockdown. Related to Figure 6.

(A) Proliferation of shRNA HHAT cancer organoids in adherent Matrigel culture compared to control cells after 6 days (mean ± SD; data from two independent experiments). ns = not significant; *p-value < 0.05; ***p-value < 0.001 (t test). (B) Fold expression of *SMO* and *PTCH1* (±95% confidence intervals) in siRNA SMO and siRNA PTCH1 transfected cancer organoids from two independent experiments. Significant differences are *p-value < 0.05; **p-value < 0.01 and were determined by inspection of error bars as described by Cumming et al. (2007) [2].

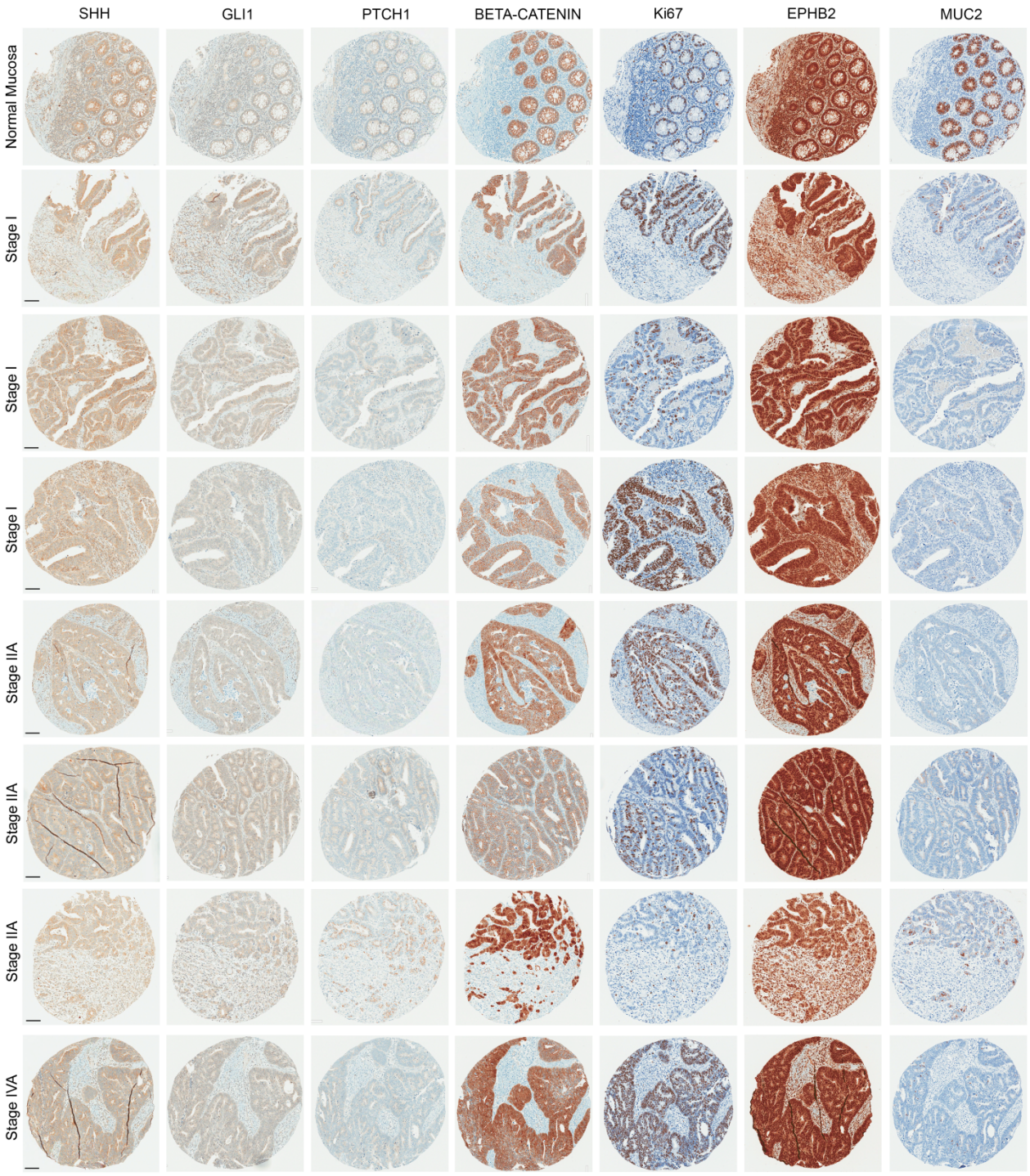

Figure S7 Immunostaining of tissue microarrays of normal intestinal mucosa and colorectal cancer patient samples for SHH, GLI1, PTCH1, BETA-CATENIN, Ki67, EPHB2 and MUC2 (Bars = 200 µm). Related to Figure 7.

Patient Model	Origin	TNM stage	Stage
281-CB-P	Transverse colon	T3 N0 M0	IIA
261-MB-P	Ascending colon	T2 N0 M0	I
162-MW-P	Sigmoid colon & descending colon	T3 N0 M0	IIA
159-MB-P	Sigmoid colon	T3 N2a M0	IIIB
238-CB-P	Sigmoid colon	T3 N0 Mx , M0	IIA
151-ML-M	Liver	T2 N0 M0 , M1a	IVA
278-ML-P	Sigmoid colon & descending colon	T4a N0 M0	IIB
302-CB-M	Liver	T3 N1a M1a	IVA
195-CB-P	Sigmoid colon	T4a N2b M1a	IVA

Table S1 Tissue Origin and TNM Classification of Malignant Tumors (TNM). Related to Figure 1.

T: primary tumor size, N: regional lymph nodes involved, M: distant metastasis

Patient Model	Gene	Description	Alteration	Amino acid exchange
281-CB-P	APC	adenomatous polyposis coli	SNV_stopgain SNV	E1379X
281-CB-P	PTEN	phosphatase and tensin homolog	SNV_stopgain SNV	R233X
261-MB-P	APC	adenomatous polyposis coli	Indel_frameshift deletion	1462_1462del
261-MB-P	APC	adenomatous polyposis coli	Indel_frameshift deletion	E1547fs
261-MB-P	APC	adenomatous polyposis coli	SNV_nonsynonymous SNV	A2690E
261-MB-P	APC	adenomatous polyposis coli	SNV_stopgain SNV	E140X
261-MB-P	BRAF	v-raf murine sarcoma viral oncogene homolog B1	SNV_nonsynonymous SNV	V600E
261-MB-P	PMS2	PMS2 postmeiotic segregation increased 2	SNV_nonsynonymous SNV	V761I
162-MW-P	APC	adenomatous polyposis coli	SNV_stopgain SNV	Q1406X
162-MW-P	APC	adenomatous polyposis coli	SNV_stopgain SNV	R876X
162-MW-P	PIK3CA	phosphatidylinositol-4,5-bisphosphate 3-kinase, catalytic subunit alpha	SNV_nonsynonymous SNV	H1047R
162-MW-P	PIK3CA	phosphatidylinositol-4,5-bisphosphate 3-kinase, catalytic subunit alpha	SNV_nonsynonymous SNV	R88Q
162-MW-P	MSH6	mutS homolog 6	SNV_nonsynonymous SNV	E948K
162-MW-P	SMAD4	SMAD family member 4	SNV_nonsynonymous SNV	D351Y
159-MB-P	APC	adenomatous polyposis coli	SNV_stopgain SNV	Q1294X
159-MB-P	SMAD4	SMAD family member 4	Indel_frameshift deletion	142_143del
159-MB-P	TP53	tumor protein p53	Indel_frameshift deletion	152_156del
159-MB-P	KRAS	v-Ki-ras2 Kirsten rat sarcoma viral oncogene homolog	SNV_nonsynonymous SNV	G13D
238-CB-P	KRAS	v-Ki-ras2 Kirsten rat sarcoma viral oncogene homolog	SNV_nonsynonymous SNV	G12D
238-CB-P	APC	adenomatous polyposis coli	Indel_frameshift deletion	N550fs
238-CB-P	TP53	tumor protein p53	SNV_nonsynonymous SNV	R273H
151-ML-M	APC	adenomatous polyposis coli	Indel_frameshift deletion	664_665del
151-ML-M	APC	adenomatous polyposis coli	Indel_frameshift insertion	I1307fs
151-ML-M	NRAS	neuroblastoma RAS viral (v-ras) oncogene homolog	SNV_nonsynonymous SNV	Q61K
151-ML-M	TP53	tumor protein p53	SNV_nonsynonymous SNV	G266E
278-ML-P	APC	adenomatous polyposis coli	Indel_frameshift deletion	K586fs
278-ML-P	APC	adenomatous polyposis coli	SNV_stopgain SNV	Q223X
278-ML-P	APC	adenomatous polyposis coli	SNV_stopgain SNV	Q223X
278-ML-P	TP53	tumor protein p53	SNV_nonsynonymous SNV	R273C
278-ML-P	PMS2	PMS2 postmeiotic segregation increased 2	Indel_frameshift deletion	287_288del
278-ML-P	PMS2	PMS2 postmeiotic segregation increased 2	Indel_frameshift deletion	287_288del
302-CB-M	PTEN	phosphatase and tensin homolog	Deletion	--
302-CB-M	APC	adenomatous polyposis coli	Indel_frameshift insertion	T1487fs
302-CB-M	APC	adenomatous polyposis coli	Indel_frameshift insertion	T1487fs
302-CB-M	KRAS	v-Ki-ras2 Kirsten rat sarcoma viral oncogene homolog	SNV_nonsynonymous SNV	G12D
302-CB-M	KRAS	v-Ki-ras2 Kirsten rat sarcoma viral oncogene homolog	SNV_nonsynonymous SNV	G12D
195-CB-P	APC	adenomatous polyposis coli	Indel_frameshift deletion	N1122fs
195-CB-P	APC	adenomatous polyposis coli	Indel_frameshift deletion	1291_1291del
195-CB-P	TP53	tumor protein p53	SNV_nonsynonymous SNV	C135F
195-CB-P	PIK3CA	phosphatidylinositol-4,5-bisphosphate 3-kinase, catalytic subunit alpha	SNV_nonsynonymous SNV	H1047R
195-CB-P	KRAS	v-Ki-ras2 Kirsten rat sarcoma viral oncogene homolog	SNV_nonsynonymous SNV	G12V

Table S2 List of major pathway mutations. Related to Figure 1.

LENTIVIRUS	SIGMA PRODUCT	PRODUCT NAME	VECTOR	TRC NUMBER
Control	SHC003V	MISSION® tGFP™ Positive Control Transduction Particles	–pLKO.1-puro-CMV-tGFP	NA
shHHAT1	SHCLNV-NM_018194	HHAT MISSION shRNA Lentiviral Transduction Particles	–hPGK-Puro-CMV-tGFP	TRCN0000422901
shHHAT2	SHCLNV-NM_018194	HHAT MISSION shRNA Lentiviral Transduction Particles	–hPGK-Puro-CMV-tGFP	TRCN0000422431
shHHAT3	SHCLNV-NM_018194	HHAT MISSION shRNA Lentiviral Transduction Particles	–hPGK-Puro-CMV-tGFP	TRCN0000422181

Table S3 Lentiviral Transduction Particles. Related to Figure 6 and 7.

TRC: The RNAi Consortium

Symbol	Gene Name	UniGene ID	TaqMan® Gene Expression Assay
ALDH1A1	aldehyde dehydrogenase 1 family member A1	Hs.76392	Hs00946916_m1
AQP3	aquaporin 3	Hs.234642	Hs01105469_g1
ASCL2	achaete-scute family bHLH transcription factor 2	Hs.152475	Hs00270888_s1
ATOH1	atonal homolog 1	Hs.532680	Hs00245453_s1
AXIN2	axin 2	Hs.156527	Hs00610344_m1
BMI1	BMI1 proto-oncogene, polycomb ring finger	Hs.380403	Hs00180411_m1
CTNNB1	catenin beta 1	Hs.476018	Hs00355049_m1
DPP4	dipeptidyl-peptidase 4	Hs.368912	Hs00897391_m1
EPHB2	EPH receptor B2	Hs.523329	Hs00362096_m1
GAPDH	glyceraldehyde-3-phosphate dehydrogenase	Hs.544577	Hs02758991_g1
HHAT	hedgehog acyltransferase	Hs.58650	Hs00911326_m1
IHH	indian hedgehog	Hs.654504	Hs00745531_s1
KRT20	keratin 20	Hs.84905	Hs00300643_m1
LGR5	leucine rich repeat containing G protein-coupled receptor 5	Hs.658889	Hs00969422_m1
MUC1	mucin 1, cell surface associated	Hs.89603	Hs00159357_m1
MUC2	mucin 2, oligomeric mucus/gel-forming	Hs.315	Hs03005103_g1
PTCH1	patched 1	Hs.494538	Hs00181117_m1
RUNX2	runt related transcription factor 2	Hs.535845	Hs01047973_m1
SHH	sonic hedgehog	Hs.164537	Hs00179843_m1
SMO	smoothened, frizzled class receptor	Hs.437846	Hs01090242_m1

Table S4 Taqman® Gene Expression Assays. Related to Figure 2, 3, 4, 5, 6 and 7.

Supplemental References

1. Schütte, M., et al., *Molecular dissection of colorectal cancer in pre-clinical models identifies biomarkers predicting sensitivity to EGFR inhibitors.* Nature Communications, 2017. **8**: p. 14262.
2. Cumming, G., F. Fidler, and D.L. Vaux, *Error bars in experimental biology.* J Cell Biol, 2007. **177**(1): p. 7-11.